GBT MEMO 188

Dynamical Rangefinder Measurements

M.A. Goldman

June 08, 1998

Abstract

This memo is an analysis of laser rangefinder measurements of reference target locations on the Green Bank Telescope, when the telescope moves.

Analysis, reduction and adjustment of range measurements to generate target locations is more complex when the telescope moves than when it is stationary. Simultaneous trilateration to a moving target by several rangefinders, is not possible. The problem of target location becomes that of acquiring ranges to distinct points along the trajectory of the target's reference point (made at different times, by several rangers) and adjusting the measured ranges to give the coordinates of the target point's trajectory versus time. This problem is not soluble without additional information!

Velocity and acceleration of the target point are, however, determined to fair accuracy by the commanded telescope pointing schedule together a model of the telescope geometry and a finite element model of the tipping structure, when significant vibration is absent. The additional velocity and acceleration information allows extrapolation of target range data acquired by different rangefinders at different times, to a common time and allows trilateration to be performed to compute target coordinates at that time.

The accuracy of target trajectory determination depends on the scan scenario used. Scan programs are defined and analyzed. Methods of range interpolation are presented. Range rate corrections to measured range distance are given.

Contents

1. Introduction

Rangefinder metrology is used to characterize the Green Bank Telescope's geometry during operation of this instrument. It is an aid to accurate determination of main reflector surface shape and telescope pointing. When measuring a telescope which is "stationary" and not driven in elevation or azimuth, rangefinder target point positions can be determined by trilaterating ranges from several rangefinders at fixed known locations. Residual target vibrational motions (excited for example by wind gusts) may be averaged by choosing appropriate integration times for range scans. Target location is essentially straightforward.

The problem becomes complicated when one ranges on the telescope while it sidereally tracks an astronomical object, performs a raster scan, or beam switches. In the latter case it is intended that laser metrology is used only for differential range measurements. But for sidereal tracking or raster scans, rangefinder coordinate trajectory measurement can be of considerable benefit. This memo examines issues relating to rangefinder metrology, both static and dynamic. It classifies the types of measurements to be made; defines the nature of the measurement process for each type of measurement; discusses range reduction and range extrapolation procedures used to compute target trajectories; discusses the

trilateration computations; provides computational methods procedures for range trajectory interpolation and extrapolation, computational procedures and finally, presents a discussion of additional problems likely to be encountered in the presence of vibrations and how they might be overcome.

The detailed program schedules for scanning multiple target by multiple rangefinders is complicated, and must be worked out in detail. Some of these details are: the interval between successive scans, target illumination interval for each scan, mutual visibility of illuminating rangefinder and target retroreflector, sequence and timing of target, calibration, and refractometer scans for each rangefinder. The relative motion between rangefinder and target during the finite range acquisition time affects the determination of target range and trajectory and must be appropriately accounted for in the coordinate determination procedure. Corrections differ for the cases of scans from ground based lasers and from feed arm lasers, and the two situations are treated separately.

Before one can use a set of measured range distances to a target to generate a target trajectory, one must first find this set of distances! A single range distance acquisition involves tracking the phase of the returned illumination signal over a finite time interval, while the target moves relative to the source (Fig. 1), and converting the time series of phases to a single measured distance at a specified "time of measurement." The computation to generate this distance and specify the time of measurement is not quite the same as the computation to generate distance to a stationary target. The stationary target distance determination is described in [Pay-1]. In this memo we discuss the determination of dynamical distance and time of measurement in the section "Reduction Of Range Measurements." We also give explicit range correction equations to provide corrections of measured range.

The method of using sets of dynamical range distances to generate computed target reference point trajectories is discussed in the section "Adjustment Of Range Measurements."

2. Types Of Measurements To Be Made

The nature of the dynamic target range measurement process and coordinate trajectory determination depends upon the site of the measuring rangefinder, the site of the target to be measured, and the type of target. Depending on the particular rangefinder and target, their relative motion may be large or small, and the prism constant correction for a cube prism target may vary or remain constant depending on whether the illumination incidence angle changes significantly during a trajectory scan. We distinguish the following cases.

Case 1.

Target Type:	Glass ball (B).	(Retrosphere).
Target Location:	Rim of main reflector.	(ZPG).
	Elevation structure.	(ZEG).
Rangefinder:	Ground.	(ZY01 - ZY12).
Relative motion of target and rangefinder.	Large.	
Prism correction:	Constant.	

Case 2.

Target Type:	Glass cube (G).	(Retrosphere).
Target Location:	Rim of main reflector.	(ZPG).
Rangefinder:	Feed arm.	(ZY13 - ZY18).
Relative motion of target and rangefinder.	Small: due to differential deformation and vibration.	
Prism correction:	Constant.	

Case 3.

Target Type:	Glass cube (G).	(Surface).
Target Location:	On main reflector surface.	(ZPG).
Rangefinder:	Feed arm.	(ZY13 - ZY18).
Relative motion of target and rangefinder.	Small: due to differential deformation and vibration.	
Prism correction:	Constant.	

Case 4.

Target Type:	Glass ball (B).	(Alidade).
Target Location:	On alidade structure.	(ZAG).
Rangefinder:	Ground.	(ZY01 - ZY12).
Relative motion of target and rangefinder.	Large.	
Prism correction:	Constant.	

Case 5.

Target Type:	Glass cube (G).	(Alidade).
Target Location:	On alidade structure.	(ZAG).
Rangefinder:	Ground.	(ZY01 - ZY12).
Relative motion of target and rangefinder.	Large.	
Prism correction:	Varies during scan.	

Case 6.

Target Type:	Glass cube (G).	(Rangefinder scan mirror).
Target Location:	On feed arm rangefinder.	(ZRG).
Rangefinder:	Feed arm.	(ZY13-ZY18).
Relative motion of target and rangefinder.	Very small.	
Prism correction:	Constant.	

Case 7.

Target Type:	Glass cube (G).	(Ground benchmark).
Target Location:	On ground monument.	(ZBG).
Rangefinder:	Feed arm.	(ZY13 - ZY18).
Relative motion of target and rangefinder.	Large.	Has motion, deformation, vibration components.
Prism correction:	Varies during scan.	

Case 8.

Target Type:	Glass cube (G).	(Subreflector).
Target Location:	On subreflector.	(ZSG).
Rangefinder:	Feed arm.	(ZY13 - ZY18).
Relative motion of target and rangefinder.	Moderate	Has Stewart platform motion and vibration components.
Prism correction:	Constant during scan.	

2.1. Ranging To The Main Reflector Rim

Six retroreflector triplet assemblies will be sited at the rim of the main reflector surface at the start of GBT telescope operation. Four more assemblies will be added subsequently. A triplet assembly consists of three reflectors, two upward-looking 2" cube corner prisms and one down-looking cat's-eye ball retroreflector. The optical fiducial reference points of the three retroreflectors lie accurately on a line. The ball reflector's center point is accurately mid-way between the fiducial points of the two cube prisms. The cube prism entry faces are mounted to point towards the centroid of the scan–mirror reference points of the 6 feed arm rangefinders. The spacing between cube prism fiducial points is accurately set and known. One can determine distance between a feed arm rangefinder and the ball retroreflector center point (which is its fiducial reference point) by ranging to the two cube prisms and then computing the median of the ranging triangle. The ball retroreflector center location can be determinated by ranging and trilateration from ground rangefinders. In this way one can provide survey ties between the ground rangefinder scan point control network and the feed arm laser scan points.

Scans in cases 1 and 2 are used to find trajectories of feed arm rangefinder scan reference points and rim ball retroreflector centers, while the telescope tracks sidereally. A time delay occurs between the scan measurements and the availability of computed trajectories. Computed trajectories are unavailable until several seconds after completion of the rangefinder scan sequence. If predicted trajectories of rangefinder reference points are available for the scheduled tracking, based on model calculations, the differences between the measured and predicted trajectories can be used to improve the model, and thereby improve the aiming codes for the feed arm rangefinders. The objective of the range measurements is to measure trajectories of the feed arm laser reference points during sidereal tracking. The measurement results are used to improve feed arm rangefinder aiming.

Each up-looking rim target prism will have an available line of sight from each feed arm rangefinder at all times. The distance between any rim prism and feed arm rangefinder will be independent of azimuth, and will have an expected total variation below 30 cm over the whole range of telescope elevation. (Figure 2).

Each down-looking rim ball retroreflector will be visible to any ground rangefinder for only a limited range of telescope elevations and azimuths. The allowable (elevation×azimuth)-space for each {ground rangefinder, rim ball} pair must be

pre-calculated using a visibility model for the ranging. Each ground rangefinder can range to a rim ball only while the ball is visible.

It may turn out to be practical to use measured trajectories of rim ball centers to provide predictive estimates of telescope pointing.

2.2. Ranging To The Main Reflector Surface

The rangefinder and target scans for case 3 are used to find the shape of the main reflector surface. Each feed arm rangefinder scans its own fixed subset of the main reflector's target retroreflectors. Targets in this subset are always visible. Targets not in this subset are never visible. Ranges from feed arm rangefinders to main surface targets are nearly independent of tipping structure azimuth and vary slowly with elevation. These ranges are expected to vary by less than 30 cm, over all elevations. Angle-of-incidence range corrections for laser beam incidence angle to the target prism face are effectively constant.

These ranges should be well-predicted by the Finite Element Model of the telescope tipping structure when the set of surface actuator settings is given.

When the telescope is stationary, with elevation and azimuth of the tipping structure held fixed, the entire set of $\simeq$ 2200 surface targets can be scanned and trilaterated. Ranges can be reduced and the trilaterations adjusted to generate a set of target locations. A best data-fit paraboloid is fitted to the adjusted positions (including the distribution of target reference point distance residuals from this paraboloid) to provide a best fit of focal length, position, and pointing of this fitted main surface shape, all within 3 to 5 minutes.

The surface can also be checked dynamically, during sidereal tracking telescope observations, by following in time (using repeated scans) the trajectories of a selected subset of $\simeq$100 surface targets. The trajectories are followed relative to the main reflector coordinate frame. The trajectory tracking measurements can provide confirmation of the surface shape during telescope tracking operation and indicate excess surface deformations, if present. Time interpolation of measured range between scans is needed, to allow range trilateration, adjustment and coor-

dinate determination.

Visibility of a feed arm laser from a surface retroreflector is found by the following method; computations are carried out in the main reflector coordinate frame. One first selects a cube corner target prism on the parent paraboloid surface, and then finds whether the line of sight from that target to each feed arm rangefinder lies within the prism's cone of visibility with respect to a unit normal vector to the prism's front (ray entry) face. One computes the direction cosines (with respect to the coordinate axes) of the unit surface normal vector (skyward) to the parent paraboloid, at the location of the target prism. One next rotates this unit vector by the offset angle of the prism's casting and calculates the direction cosines of the (skyward) unit normal to the prism's front face. Finally, one calculates the unit direction vector from the prism towards each rangefinder. The cosine of the angle which this direction vector makes with the unit normal to the prism front face is just the dot product of these unit vectors. The direction ray from prism to rangefinder lies within the prism's cone of visibility if the cosine just computed is greater than the cosine of the half-angle of the cone of visibility, that is the angle of the ray from target to rangefinder from the prism face normal is less than the visibility cone's half-angle.

The return response of a glass cube corner prism drops off sharply with increasing angle of incidence [Rüe-1]. The return drops sharply between twenty and thirty degrees incidence angle. The effective half cone angle at the target for visibility of the rangefinder is approximately 25 degrees. Some return may be expected up to 40 degrees.

2.3. Ground Ranging To The Elevation Structure

During ranging from ground rangefinders to targets on the elevation structure (Figure 3) large scale relative motion occurs between rangefinder and target. Visibility changes. If the target is a cube corner reflector, the incidence angle of target illumination also changes.

Algorithms used for time extrapolation of range distances and for trilateration computations of target trajectories must be examined carefully to insure that their error bounds are acceptably small.

2.4. Ground Ranging To The Alidade Structure

Distance measurements from ground rangefinders to alidade structure targets, cases 4 and 5, are made to obtain information about large scale motions of the alidade structure and the orientation and position of the elevation axis of the telescope. Stationary measurements are made to determine alidade position and orientation versus azimuth to determine alidade track contributions to pointing error. A program of stationary measurements is to be carried out to study thermal and wind-loading effects on the alidade structure. Stationary range measurements to ball retroreflectors sited beneath the elevation bearings will be made, to estimate elevation axle tilt, orientation and position versus azimuth and tipping-structure-elevation, to provide estimates of corrections to be made for pointing and focus tracking. Dynamic measurements to the alidade structure are expected to be rare. To schedule, analyze and evaluate such dynamic measurements presents the same problems as for range measurements to rim ball targets, and is done in the same manner.

2.5. Distance Measurements Between Rangefinders

A special measurement situation occurs when ranging from a rangefinder to a second, target, rangefinder. Distance from the scan-mirror reference point of the illuminating rangefinder to the scan point of the illuminated rangefinder is to be measured. A direct measurement between scan points is not possible. Instead,

one measures from the scan point of the source rangefinder to the fiducial reference point of a cube corner retroreflector joined to the back of the target rangefinder's scan mirror; the targeted rangefinder's scan mirror is flipped, to expose its retroreflector and is aimed to face the source rangefinder (anti-autocollimation position). Range is measured between the scan point of the illuminating rangefinder and the fiducial reference point of the exposed cube prism on the targeted rangefinder. That measured range is then corrected to account for the vector displacement of the target retroreflector's reference point from its own scan-mirror reference point.

The scan program for such a measurement must include special instructions to flip and aim the scan mirror of the target rangefinder so that its attached cube reflector faces the source laser (near zero angle incidence). It must also allot time for a handshake between the ZY-computers of thetwo rangefinders and the ZIY metrology system computer. This hand shake is an exchange of signals to notify of readiness for scan and an acknowledgement of permission to scan. The range reduction computation must include the special correction above, to account for displacement of the target retroreflector's fiducial reference point from its own scan-mirror's reference point.

The range correction geometry is shown in Fig. 5. By manufacture, the entry face of the retroreflecting cube corner prism on the back of the scan mirror is accurately parallel to the rangefinder's scan-mirror surface plane. Let $(H)_j$ be the distance between the entry face plane of the prism and the plane of the scan mirror. (This is easily measured using gauge blocks). Let $(D)_j$ be the depth of the target prism, and n be the group index of the prism glass divided by that of air at 780 μm wavelength. Then if R_{true} is the range between the scan mirror reference points of the source and target rangefinders and R_{meas} is the measured range between the illuminating rangefinder's scan point and the prism target reference point,

$$(2.5.1) \qquad R_{true} = R_{meas} + (H)_j - \frac{(D)_j}{n} .$$

If the prism entry face is not perpendicular to the line between scan reference point centers, but is tilted by an angle I_{in}, so that the laser radiation is incident at angle I_{in} to the normal to the prism entry face (Fig. 6), the range R_{true} may be found from the law of cosines,

$$(2.5.2)\quad R_{meas}^2 = R_{true}^2 + \left((H)_j - \frac{(D)_j}{n}\right)^2 - 2\cdot R_{true}\cdot\left((H)_j - \frac{(D)_j}{n}\right)\cdot\cos I_{in}\ .$$

In equation (2.5.2) it is assumed that the measured range R_{meas} has itself already been corrected for the non-zero incidence angle I_{in}, using the static incidence angle correction given by equation (A4.1) of GBT Memo 154 [Gol-2].

In general one sets the target rangefinder's scan mirror within minutes of arc to face the source rangefinder, so the correction (2.5.1) is sufficient. Only in the rare case that one must simultaneously scan a target rangefinder by two source rangefinders will (2.5.2) be used.

An important case of rangefinder-to-rangefinder measurement occurs when the main reflector surface shape is to be determined. A local control network of feed arm rangefinder scan reference point positions is needed, to determine surface target positions by trilateration. This network of control points is established by scans between feed arm rangefinders, before trilaterating.

2.6. Other Distance Measurements From Feed Arm Rangefinders

Dynamical measurements from feed arm rangefinders to targets on the subreflector structure present additional complication. To aim the rangefinders, the *a-priori* schedule of tracking motion of the subreflector (Stewart platform drive) during the observing run should be made available to the feed arm ZY-computer aiming clients. Finite element estimates of upper feed arm bending corrections to rangefinder aiming should also ber supplied. The latter corrections may be small, because the distances from feed arm rangefinders to the subreflector are of order 20 meters, and the feedarm is relatively rigid locally over this distance scale.

For closed servo loop observing (Phase III), additional complications arise. Considerations of ambiguity, multiple solutions, subreflector servo drive instability, and other potential problems will have to be identified and analyzed in detail, before one dares to attempt focus tracking using rangefinders within a closed servo loop. Separate range adjustment codes are required.

These issues are of too great a complexity to be approached in this memo and are left for separate, future analysis.

3. The Measurement Process

3.1. Description Of The Scanning Procedure

Parameters related to the procedures for range distance measurement are included in Table I. The computational modules named in capital letters are to be resident in the ZY and ZIY metrology system computers, and are still under development. Their functionality and inter-relationships are outlined in the GBT Laser Ranging System Metrology Interface Configuration Diagram, GBT Drawing No. D35420K014 [Gol-3]

Dynamical scanning is done as follows. One starts with a telescope observing run schedule. A server from the "Pointing Model" of the telescope delivers a schedule of commanded telescope elevation angle and azimuth angle settings versus time, and their first and second time derivatives to a client "RANGEFINDER ATTITUDE COMPUTATIONAL PROCESSOR" resident in the host ZY-computer of each rangefinder. That processor computes local rangefinder drive encoder count settings used to aim the rangefinder. Algorithms used for rangefinder aiming, including telescope structure gravity deformation corrections from the Finite Element Model of the tipping structure, are outlined in GBT Memo 165 [Gol-1].

To initiate any range scan program, the program must be requested and scheduled. The name of the requested range scan program and its start clock time are entered as a request to a "SCHEDULER FOR RETROREFLECTOR SCANS." The program request can be made by keyboard entry to a telescope control room computer keyboard, aided by a graphic user monitor interface: "TELESCOPE OPERATOR INITIATED SCHEDULING REQUESTS." This interface will pass the program request to the GBT metrology system ZIY-computer. That computer will coordinate the implementation of the scan program with the ZY_i computers at the individual rangefinders, which will do most of the actual pre-scan computation, scan trigger generation, scan drive motor control, range acquisition, and range data pre-processing. The reduction of electronic phase data to generate ranges will be performed in each ZY_i-computer, which will store the unadjusted range information (for the scans of that ZY_i rangefinder) as output range data vectors internally in an "UNADJUSTED MEASURED RANGES DATA BUFFER /

ZY_i." The output range data vectors will also be passed from each ZY-computer to the ZIY-computer, which will store the entire set of unadjusted ranges in a data buffer: "UNADJUSTED MEASURED RANGES DATA BUFFER / ZIY." Range adjustments will be generated in the ZIY-computer by resident "RANGE ADJUSTMENT CODES" and stored in the "ADJUSTED RANGE AND FIDUCIAL POINT COORDINATE DATA OUTPUT FILE BUFFER." If a request has been previously been entered as a telescope operator initated scheduling request or as an active surface module initiated scheduling request, the adjusted range and coordinate data will be copied to a named data log archive file.

When requesting initiation of a range scan program, one can request data-archiving of the scan program measurement results to one or more data log archive files by using a sub-interface of the telescope operator initiated scheduling requests: "TELESCOPE OPERATOR INITIATED REQUEST SCHEDULER FOR DATA ARCHIVE."

As part of the telescope's operation, scheduled elevation and azimuth angles versus time will be delivered by the telescope's commanded track server to a client "LINE OF SIGHT VISIBILITY COMPUTATION PROCESSOR" resident in each ZY_i-computer. This processor is a pre-scan filter. It decides whether a scheduled scan should actually be made from that rangefinder to any particular target (of a type pre-scheduled before the observing run), governed by their mutual visibility at the telescope azimuth and elevation during the scan. The processor modifies the scan list to carry out only scans which can possibly succeed, and computes aiming coordinates only for acceptable scans. Subsequently, the start and stop and event trigger times times for each allowed scan are computed, either in this processor or another.
The ZY_i-host computer generates a double loop of scans (Figure 4):

1. It updates the list of visible targets, ranger scan drive coordinates, and scan start, stop and event trigger times for the next scan sequence.

2. It commands a scan of the ranger's local calibration reference range retroreflector, to obtain the calibration range correction parameters, used for this scan loop.

3. If this ranger is to scan a refractometer target as part of the scan loop,

it generates trigger signals to scan the refractometer target.

4. It sequentially scans each of the listed targets in the scan loop (first run through the inner loop).

5. It repeats the scan of listed targets (runs through the inner loop until a pre-specified number of inner loop cycles is run).

6. It repeats the double loop starting at 1. until a stop command is given.

A server is resident in each ZY_i-computer to set externally generated scan options, the "SCHEDULER FOR RETROREFLECTOR SCANS." The client sources commanding these scans are varied. For example one might follow a sequence of surface scans by a sequence of subreflector scans or might wish to interleave surface and ground benchmark target scans. The scan parameters for the varied scan sequence scenarios for the individual rangefinders are to be resident in the rangefinder's ZY_i-computer scheduler for retroreflector scans. Requests by external clients: the active surface module, focus tracking module, or telescope-operator- initiated requests, will be routed through the ZIY metrology system computer These external clients are the ultimate sources of scan requests for the rangefinders.

The inner and outer loop scan cycles described in Fig. 4 are characterized by the inner and outer loop cycle repetition times Δt_{cyt} and Δt_{cy}. One may want to perform a rapid repetitive sequence of measurements to certain targets to generate those targets' trajectories, while measurements to other targets may be needed less frequently. The double loop scan procedure may be more convenient to implement than to use a just a single loop with repeated scan commands to individualtargets.

The scheduler for scans in each ZY-computer also generates event triggers to control individual scans (Fig. 8). If the time between successive scans of a rangefinder is h $(= \Delta t_{cyt})$, the mid-scan time of the next scan is t, and the scan integration time interval is Δt_i, the scheduler provides triggers to initiate the following events: stop laser illumination for the previous scan, at time $t - h + \frac{\Delta t_i}{2}$; command and control the rangefinder motor drive during a time interval Δt_{md} allotted to aim and drive the ranger's scan-mirror to its next scan position; confirm scan readiness by the ZY-computer and get a consent-to-scan

reply from ZIY during an allotted "handshake" time interval Δt_{hs}; start laser illumination for the next scan, at time $t - \frac{\Delta t_i}{2}$. The inter-scan time intervals are subject to the constraint: $\Delta t_i + \Delta t_{md} + \Delta t_{hs} < h$.

We next discuss methods to reduce scan measurement data, to generate range distance versus time. The variables appearing in the range reduction computations are listed in Appendix F.

3.2. Range Measurement Reduction

A range measurement is a determination of distance between two points in space, at a given time. For our purposes, these are the rangefinder scan fiducial reference point and the target fiducial reference point. The points are each embedded in a real physical body. The scan reference point sits in the surface of the rangefinder's scanning mirror, at the intersection of the rangefinder drive axes (contrived to intersect at a point on the mirror surface). The retroreflector fiducial point is fixed either inside a cube corner prism or at the center of a glass ball [Peck-1, Gol-1, Rüe-1].

The theory of rangefinder operation, and method of determining range when both rangefinder platform and target are stationary is discussed by Payne, Parker and Bradley [Pay-1] and by Hashemi, Hurst and Oliver [Has-1]. We extend these treatments to the case when the two points are in motion with respect to one another.

By "range measurement reduction" we refer to the process of converting a time-averaged electromagnetic phase delay, obtained for a measurement involving a scan reference point S_i of rangefinder ZY_i and a retroreflector target fiducial point T_j, to a pair of real numbers: d_{ij} , t_{ij} . The first number is the "measured distance between S_i and T_j." The second number is the "time at which the distance is measured." We also refer to this pair as $d(S_i, T_j; t)$.

In reality, the measurement process takes a finite time to complete, the "scan measurement time" or integration time, Δt_i. The process of measurement occurs over a time interval starting at time $t_{ij} - \Delta t_i/2$ and ending at time $t_{ij} + \Delta t_i/2$. The procedure for converting phase to distance is discussed in [Pay-1] for static measurements. When the telescope moves, both the target and rangefinder fiducial points may move.

In order to aim the rangefinder from S_i to T_j at time $t_{ij} - \Delta t_i/2$ one must compute the coordinates of the range pair points at some time in the interval $t_{ij} - \Delta t_i/2$ to $t_{ij} + \Delta t_i/2$. To do this one uses the available commanded track state vector values of commanded azimuth and commanded elevation of the telescope, and

their time derivatives, together with current tabulated data base values of geometric elevation frame coordinates to calculate *a-priori* estimated coordinates of the range pair points using the Finite Element Model for the telescope. One also calculates an *a-priori* estimated range distance $d_{ij}(AZ_{com}(t_{ij}), EL_{com}(t_{ij}))$. This estimated distance is used, with a correction term (to be discussed) to provide the modular range distance $\mathcal{N}_{ij} \cdot \left(\frac{\lambda_{\text{mod}}}{2}\right)$ in integral multiples of the modulation half-wavelength.

Conversion of measured phase information to produce $d(S_i, T_j; t)$ requires independently obtained *a-priori* knowledge of the relative motion of S_i and T_j. Propagation phase delay information is acquired during the whole of the scan measurement time. Fortunately, we will usually have a measurement situation where relative motion varies smoothly, accelerations are small, and relative radial velocities and accelerations are known to moderate accuracy in advance. Because these special conditions exist, it then becomes possible to obtain a value for $d(S_i, T_j; t_{ij})$ and to interpolate it for short time increments to get a value for $d(S_i, T_j; t)$ when t is near t_{ij} .

During open loop sidereal tracking while beam switching and wind gust induced oscillations are absent, target rangefinder scan point velocities and accelerations are determined sufficiently accurately by the telescope azimuth and elevation angle drive schedules and their first and second time derivatives. Commanded azimuth and elevation encoder angles and their time derivatives determine the velocity and acceleration vectors of feed arm laser scan points and tipping structure and surface retroreflector target fiducial points via the geometric telescope model plus Finite Element Model deformations. Given these commanded angle schedules, one uses the time derivatives of known coordinate transformation matrix functions of elevation and azimuth to obtain derivatives of range with time and then correct the computed range. It will be demonstrated, in Appendix A, that target-rangefinder Doppler corrections are sufficiently small to be ignored. Relative acceleration between scan rangefinder and retroreflector target during the range measurement time Δt_i produces a range increment, however, which must be included in the range reduction.

During open loop dynamical scanning of surface or rim targets by feed arm lasers, relative motion corrections are due to differential motions caused by feed

arm bending. This is estimated by quasi-static calculations. One computes feed arm bending deformations as determined statically by the Finite Element Model and using elevation angle rate of change as determined by the elevation encoder drive schedule. These computations are performed in the rangefinder attitude computational processor resident in each ZY-host computer.

During open loop dynamical scanning of subreflector targets by feed arm lasers, relative motions are due to differential motion caused by feed arm bending together with differential subreflector motions due to scheduled rotation and translation of the subreflector (generated by driving its Stewart platform actuators). These additional scheduled subreflector motions should be included in the dynamic relative velocity and acceleration range corrections.

The detailed computations for driven motion corrections are not included in this memo.

3.3. Range Measurement Adjustment

By "adjustment of a set of range measurements" we refer to the process of using a set of measured ranges made at arbitrary times (by some subset of the rangefinders) to a particular retroreflector target, to provide an estimated trajectory of the target, together with error estimates and error bounds for the computation. That is, one calculates coordinates of a target reflector's fiducial reference point as functions of time. The coordinates may be either in the ground frame or the geometric elevation frame of reference. Often, the trajectory motion is smaller in the elevation frame and it is advantageous to convert coordinates to this frame and then perform the adjustments in this frame.

When the rangefinder platforms and reflector target do not move, one merely trilaterates an overdetermined set of range distance data. This is an ordinary least squares survey adjustment, done by setting up and solving the normal equations for the set of measured distances. The solution produces a set of best-estimate coordinates, together with a standard error for each coordinate. In this situation the target trajectory is a fixed point.

For example, input data for this trilateration could be the ground frame X, Y, Z

coordinates of the ground rangefinder scan points and their a-priori standard errors as determined by a control survey, and the set of reduced range distances to an observed retroreflector target's fiducial point. This data can be reduced by commercially available codes (e.g. STAR NET). The adjustment codes generate adjusted range distances, together with the adjustment standard errors, and also adjusted ground frame coordinates of the target's fiducial point, together with the standard error of each coordinate.

A closely related situation occurs when the rangefinder platforms are stationary and the telescope is not being driven by its azimuth and elevation motors, but the target vibrates due to wind gusts. One can still use trilateration in this situation, if one is careful in one's choice of measurement procedure. The rangefinders can alternate scans with long integration times with scans of short integration time. Long integration time scan observations give the mean target range by averaging. Short integration time scans provide sufficient data to follow and record the oscillating components of target motion, giving frequencies, amplitudes and phases of its oscillation modes. One trilaterates the mean ranges to obtain the mean target coordinates. The projections of the oscillating target motions along the directions of the individual scan point to mean-target directions are then available and one can then use the short integration time range data to solve for the oscillatory motions. It is conceivable that in certain particular cases one might also acquire additional data from accelerometers on the telescope.

When targets or rangefinder platforms move, the problem is more complex. One cannot range on a moving target with four or more lasers simultaneously. Generally, during ranging on a moving target, the scanning rangefinders acquire their data at different times. A rangefinder will scan each target repetitively. Each range scan requires a finite time, Δt_i, to acquire range distance data; this data must be processed to subsequently provide a good value of range distance to the moving target at some time during the scan. Similar considerations arise when rangefinder platforms move, and range to moving targets on the telescope or to fixed benchmark reflectors on the ground. The problem of adjusting the measurement data is insoluble, because the trajectories of the target and laser scan points are not, in fact, determined by the measurements! One needs additional information about rangefinder and target motions to define their trajectories.

The velocity and acceleration trajectories of a target retroreflector are gen-

erated by programmed drive motions, by quasi-equilibrium deformation of the telescope structures, and by wind or dynamically excited vibrations. The first two of these, the major contributors to target motion, can be predicted from the available programmed azimuth and elevation drive schedule for observing, using the geometric model of the telescope and the finite element model of the telescope structure. The schedule for commanded pointing provides advance information giving the commanded azimuth and elevation angles and their first two time derivatives. This information is available for improvement of rangefinder aiming, prior to scan.

Vibrational motion is significant primarily for targets on the feed arm and subreflector. Vibration contributions could, in principle, be obtained from acceleration measurements made by multi-axis accelerometers on the feed arm and subreflector. They would not be known *a-priori* but would be available later for post-processing of the range measurement data.

Subreflector motions have an additional cause, the driven commanded track motions of the Stewart platform actuators. Subreflector retroreflector target velocities and accelerations can be computed *a-priori* given the commanded track schedule for the subreflector actuators and the pointing schedule. For open loop drive of the subreflector such correction is relatively straightforward. If the subreflector is intended to be used in closed loop operation, with position pickup from the laser rangefinders, the design of such a feedback control will be complex, and must be done carefully to avoid feedback instability. The considerations for closed loop subreflector control are beyond the scope of this note, and are not approached here.

References

[Cre-1] R.E. Creager, *The Green Bank Telescope Laser Metrology System, ZIY Version 2.5 Software Interface Reference Manual,* NRAO Green Bank, February 12,1998.

[Gol-1] M.A. Goldman, *GBT Coordinates And Coordinate Transformations*, GBT Memo 165, February 1997.

[Gol-2] M.A. Goldman, *GBT Dish Laser Range Measurement Corrections*, GBT Memo 154, June 1996.

[Gol-3] M.A. Goldman, Laser Ranging System Laser Metrology Interface Gonfiguration Diagram. GBT Drawing No. D35420K014. May 23, 1997.

[ESA-1] Explanatory Supplement to the Astronomical Almanac, Edited by P.K. Seidelmann. Chapter 11. University Science Books, Mill Valley CA, 1992.

[Has-1] K.S. Hashemi, P.T. Hurst, J.N. Oliver, *Sources Of Error In A Laser Rangefinder*, Rev. Sci. Instrum. 65(10), October 1994.

[Hil-1] F.B. Hildebrand, Introduction To Numerical Analysis. McGraw-Hill, New York 1956. Chapter 4.

[IEEE-1] IEEE Transactions on Automatic Control, Special Issue on Applications of Kalman Filtering, Vol. AC-28, No. 3, March 1983.

[Pay-1] J.M. Payne, D. Parker, R.F. Bradley, *Rangefinder With A Fast Multiple Range Capability,* Rev. Sci. Instrum. 63(6), June 1992.

[Par-1] D.H. Parker, *Draft Notes On The Green Bank Telescope Laser Metrology System,* NRAO Green Bank, January 28,1996.

[Pec-1] E.R. Peck, *Theory Of The Cube Corner Interferometer,* J. Opt. Soc. Am. 38(12), December 1948.

[Pre-1] W.H. Press, B.P. Flannery, S.A. Teukolsky, W.T. Vetterling, *Numerical Recipes in C,* Cambridge Univ. Press, 1988. Sections 3.1, 3.2.

[Rüe-1] J.M.Rüeger, *Electronic Distance Measurement,* Chapter 10. Springer-Verlag, New York, 1989.

[Wel-1] D. Wells, More About The Closed-Loop Surface Servo, Private memo, June 9, 1997.

Appendix A. Dynamical Range Distance Correction.

Here we compute the return signal from a linearly moving non-rotating prism retroreflector to a stationary source. In this appendix we use the following convention: the index i refers to an illuminating rangefinder; the index j refers to a target retroreflector prism; in the special case that the target retroreflector is a prism attached to the scan mirror of a rangefinder we use the index i' to refer to this prism.

We make the following assumptions:

1. The signal source is stationary. The target moves on a line. The distance between source and target is a smooth function of time, possessing derivatives of all orders.

2. The source is assumed to continuously generate a modulation signal:

$$\text{(A.1)} \qquad e_S(t) = \cos(\omega_{\text{mod}} \cdot t)$$

travelling at speed $\frac{c}{\eta}$ where c is the speed of light in vacuum and η is the group index of refraction in air at 780 μm wavelength.

3. Target prism, $T(j)$, is non-rotating and is oriented with its entrance face perpendicular to the line of motion. The prism depth is $(D)_j$. The group refractive index of the prism glass is assumed to be η_{glass}. Define the ratio of the group indexes, glass to air, as $n = \frac{\eta_{glass}}{\eta}$. We define the distance d_T of the target fiducial point T_j from the prism entry face, the prism correction constant $(P_c)_j$, and the one-way propagation delay time in glass τ_g respectively by

$$\text{(A.2)} \quad d_T = \frac{(D)_j}{n}\,; \quad (P_c)_j = -(D)_j \cdot (n - \frac{1}{n})\,; \quad \tau_g = \frac{(D)_j \cdot \eta_{glass}}{c}\,.$$

For BK7-glass, $\eta_{glass} = 1.527643$ at 780 μm. To sufficient accuracy for our purposes, we use $n = 1.527077$ to make the prism correction. (For our short prism depth, we use a nominal value $\eta = 1.000253$ to compute the prism correction but use values corresponding to current meteorological measurements to correct propagation range). For a sample of 162 main reflector surface cube corner prisms, the

mean depth D was 0.742" . (For this mean value of prism depth, $P_c = -0.6472$").

4. The signal received at the rangefinder, at time t, is a non-attenuated replica of the signal emitted at time $t - \tau_p(t)$. Here $\tau_p(t)$ is the round-trip propagation delay of the signal returning to the rangefinder at time t; the delay $\tau_p(t)$ will have to be computed from knowledge of the target velocity and acceleration during some time interval prior to t. Explicitly, we assume that

$$(A.3) \qquad e_R(t) = e_S(t - \tau_p(t)) = \cos(\omega_{\text{mod}} \cdot (t - \tau_p(t))).$$

5. We assume that the received signal will be compared to the source signal during the time interval from $t^0 - \frac{\Delta t_i}{2}$ to $t^0 + \frac{\Delta t_i}{2}$. During this integration time, Δt_i seconds long, we assume that the actual distance $d(t)$ of the target from the source is described by a finite Taylor's series expansion with remainder term, centered at the middle of this time interval:

$$(A.4) \quad d(t) = d_0 + (\dot{d})_{t^o} \cdot (t - t^0) + (\frac{1}{2!})(\ddot{d})_{t^o} \cdot (t - t^0)^2 + \cdots + (\frac{1}{m!})(\frac{d^{(m)}d}{dt^m})_\theta \cdot (t - t^0)^m , \qquad (t^0 - \frac{\Delta t_i}{2} < t < t^0 + \frac{\Delta t_i}{2}).$$

The derivatives of distance with time are obtained from other sources of information about the relative radial motion between source and target, and are assumed to be available *a-priori*. Calling

$$(A.5) \qquad v_o = \frac{d}{dt}(d(t))_{t^0} , \quad a_o = \frac{d^2}{dt^2}(d(t))_{t^0} , \quad k_o = \frac{d^3}{dt^3}(d(t))_{t^0} ,$$

we can write (A.5) in the form

$$(A.6) \quad d(t) = d_0 + v_o \cdot (t - t^0) + (\frac{a_o}{2}) \cdot (t - t^0)^2 + (\frac{k_o}{6}) \cdot (t - t^0)^3 + \text{ higher order terms.}$$

The propagation delay term is computed as follows. The signal modulation propagates at the group speed $\frac{c}{\eta}$ in air. The round-trip propagation delay interval is exactly twice the one-way propagation delay. The propagation delay is the sum

of the delays in air and in glass. We then get

$$\text{(A.7)} \qquad \tau_p(t) \;=\; 2(\frac{\eta}{c})\cdot\{d(t-\frac{\tau_p(t)}{2})-d_T\}+2\cdot\tau_g\ .$$

This is the basic functional equation used to compute the dynamical propagation delay. We use it, together with *a-priori* information available on the target motion to find the propagation delay $\tau_p(t)$ in terms of the range distance and its derivatives at the middle of the integration interval. Subsequently, we can compute dynamical corrections to the measured range due to the target motion.

To compute $\tau_p(t)$ we define the one-way propagation distance corresponding to the signal received at time t. Let

$$\text{(A.8)} \qquad y \;\equiv\; (\frac{c}{\eta})\cdot(\frac{\tau_p(t)}{2}),\quad \text{which gives} \quad \frac{\tau_p(t)}{2} \;=\; \frac{\eta y}{c} \quad \text{and}$$

$$\text{(A.9)} \qquad t-t^0-\frac{\tau_p(t)}{2} \;=\; t-t^0-\frac{\eta y}{c}\ .$$

Using (A.5) and (A.6), functional equation (A.7) takes the form

$$\text{(A.10)} \quad y \;=\; d_0-P_c+v_o(t-t^0-\frac{\eta y}{c})+\frac{a_o}{2}(t-t^0-\frac{\eta y}{c})^2+\frac{k_o}{6}(t-t^0-\frac{\eta y}{c})^3+\cdots .$$

Expanding the terms in parentheses gives

$$\text{(A.11.1)} \qquad y \;=\; d_0+|P_c|+v_0\cdot(t-t^0)+\frac{a_0}{2}\cdot(t-t^0)^2+\frac{k_0}{6}\cdot(t-t^0)^3+\cdots$$

$$-(\frac{\eta y}{c})\left[v_0+a_0(t-t^0)+\frac{k_0}{2}(t-t^0)^2\right]+(\frac{\eta y}{c})^2\left[\frac{a_0}{2}+\frac{k_0}{2}(t-t^0)\right]+(\frac{\eta y}{c})^3\left[\frac{k_0}{6}\right]+\cdots .$$

This gives

$$\text{(A.11.2)} \quad y=\frac{d_0+|P_c|+v_0\cdot(t-t^0)+\frac{a_0}{2}\cdot(t-t^0)^2+\frac{k_0}{6}\cdot(t-t^0)^3+\cdots}{1+(\frac{\eta}{c})\left[v_0+a_0\cdot(t-t^0)+\frac{k_0}{2}\cdot(t-t^0)^2\right]+\mathbf{O}\left[(\frac{\eta}{c})^2\right][y\cdot a_0+\cdots]}\ .$$

Under operating conditions of the telescope and rangefinder system we have the following limits on the operating parameters:

(A.12) $d_0 < 200$ meter, $\quad |v_0| < 0.5$ meter/sec, $\quad |a_0| < 0.1$ meter/sec^2.

During a scan measurement, the term $(t - t^0)$ is no larger than $\Delta t_i/2$, half the individual scan integration time interval. Dynamic scan integration intervals are typically 1/16 second or less. For such short intervals, contributions of jerk and higher order terms are small. Under these conditions, terms in the denominator of equation (A.12) reduce to unity without introducing error more than a few microns. To sufficient accuracy (for our purposes), we can use

$$(A.13) \qquad y = d_0 + |P_c|_j + v_0 \cdot (t - t^0) + \frac{a_0}{2} \cdot (t - t^0)^2 \ .$$

From the definition $\tau_p(t) \equiv \dfrac{2\eta y}{c}$ and (A.3) we get

$$(A.14) \quad e_R(t) = \cos \omega_{\text{mod}} \left\{ t - (\frac{2\eta}{c}) \left[d_0 + |P_c|_j + v_0(t - t^0) + \frac{a_0}{2}(t - t^0)^2 \right] \right\}.$$

It is convenient to normalize distance to units of a modulation half-wavelength,

$$(A.15) \qquad \frac{\lambda_m}{2} \equiv \frac{(2\pi) \cdot c}{2 \cdot \omega_{\text{mod}}} \qquad (= 0.099930819 \text{ meter}).$$

The received signal is then

$$(A.16) \quad e_R(t) = \cos \left\{ \omega_{\text{mod}} \cdot t - (2\pi) \cdot \eta \cdot \left[\frac{d_0 + |P_c|_j + v_0 \cdot (t - t^0) + \dfrac{a_0}{2} \cdot (t - t^0)^2}{(\lambda_m/2)} \right] \right\}.$$

We have not yet separated out the propagation delay due to common mode propagation path. The total propagation path includes not only the 2-way path from rangefinder mirror scan point S_i to retroreflector target reference point T_j, but also includes the sum of two 1-way paths: from the laser junction to the scan point, and from the scan point to the photodetector focus. We call the mean of these two 1-way paths $(L_{cmm})_i$.

Let us split the range distance into two parts:

(A.17) $\quad d(t) = d_{ij}(t) + (L_{cmm})_i \,, \quad d_0 = d(t = t^0) = d^0_{ij} + (L_{cmm})_i \,.$

Here, d^0_{ij} is the actual geometric distance from the rangefinder scan reference point to the target reference point at time t^0, and does not include $(L_{cmm})_i$, the common mode optical path divided by η.

We now express distance in terms of a normalized optical path

(A.18) $\quad \mathcal{S}_{ij} \equiv \dfrac{\eta \cdot (d^0_{ij} + |P_c|_j + (L_{cmm})_i)}{(\lambda_m/2)}$ and parameters

(A.19) $\quad f_v \equiv \dfrac{2 \cdot \eta \cdot v_0}{\lambda_m} \quad , \quad h_a \equiv \dfrac{\eta \cdot a_0}{\lambda_m} \,.$

The received signal is

(A.20) $\quad e_R(t) \;=\; \cos\left\{\omega_{\text{mod}} \cdot t - (2\pi)\left[\mathcal{S}_{ij} + f_v \cdot (t - t^0) + h_a \cdot (t - t^0)^2\right]\right\} \,.$

Signal $e_R(t)$ is modular in $\mathcal{S}_{ij}$ with period 1, and in optical path with period $(\dfrac{\lambda_m}{2})$.

We partition the 1-way optical propagation path length into four path lengths, and scale path length in units of the modulation half-wavelength. The first length is

(A.21) $\quad \mathcal{N}_{cmm} = \text{Int}\left\{\dfrac{\eta \cdot (L_{cmm})_i}{(\lambda_m/2)}\right\}.$ The second is

(A.21.1) $\quad (D_{cmm})_i = \left[\dfrac{(\eta \cdot (L_{cmm})_i \;-\; \mathcal{N}_{cmm} \cdot (\lambda_m/2))}{(\lambda_m/2)}\right] ,$

where $0 \leq (D_{cmm})_i < 1$.

The scaled length residual $(D_{cmm})_i$ is a property of the rangefinder, and is almost independent of atmospheric refraction, because L_{cmm} is short. It can be measured in the laboratory for each rangefinder and used as a calibration parameter for that rangefinder. We assume that this parameter is available in the rangefinder correction parameter data base. (An approximate value is sufficient for our needs).

The third length is $\mathcal{N}_{ij} \cdot (\frac{\lambda_m}{2})$, the largest integer multiple of $\frac{\lambda_m}{2}$ within the approximate optical propagation path length: from S_i to T_j plus the residual modular length of the rangefinder calibration path.. (The approximate optical path length from S_i to T_j is the tabulated approximate distance between these points plus the amplitude of the prism correction constant of the target prism, multiplied by the group index η of air).

The fourth length is a residual of that path, $D^0_{ij} \cdot (\frac{\lambda_m}{2})$.

That is, there exists a unique positive integer, $\mathcal{N}_{ij}$, and a residue, D^0_{ij} $(0 \leq D^0_{ij} < 1)$, such that:

$$\text{(A.22)} \qquad \eta \cdot (d^0_{ij} + |P_c|) \; + \; (D_{cmm})_i \cdot (\frac{\lambda_m}{2}) \; = \; \mathcal{N}_{ij} \cdot (\frac{\lambda_m}{2}) + D^0_{ij} \cdot (\frac{\lambda_m}{2}) \,, \quad \text{with}$$

$$\text{(A22.1)} \quad \mathcal{N}_{ij} \; = \text{Int} \left\{ \frac{\eta \cdot [\; d_{ij}(AZ, EL) + \; | \; P_c \; |_j]}{(\lambda_m/2)} \; + (D_{cmm})_i \right\} \quad \text{so that}$$

$$\text{(A.22.2)} \qquad d^0_{ij} = (\frac{1}{\eta}) \left\{ (\mathcal{N}_{ij} + D^0_{ij} - (D_{cmm})_i) \cdot (\frac{\lambda_m}{2}) \right\} - |P_c|_j \; .$$

where $0 \leq D^0_{ij}$, $(D_{cmm})_i < 1$ and $\mathcal{N}_{ij}$, $\mathcal{N}_{cmm}$ are positive integers.

The nominal distance $d_{ij}(AZ, EL)$ is obtained by looking up the geometric elevation frame coordinates of S_i and T_j from the telescope geometry data base, correcting them for telescope elevation EL using the Finite Element Model of the tipping structure, and then computing the distance between the gravity-shifted positions of the two points.

The measured range path is then

$$\text{(A.23)} \quad \mathcal{S}_{ij} \cdot (\frac{\lambda_m}{2}) = \eta \cdot (d^0_{ij} + |P_c|_j + (L_{cmm})_i) = (\frac{\lambda_m}{2}) \cdot \left(\mathcal{N}_{cmm} + \mathcal{N}_{ij} + D^0_{ij} \right) .$$

The optical path residual D^0_{ij} is an unknown, to be found by the rangefinder scan, to complete the measurement of range. In terms of the optical path residuals, the received range signal can be written as

(A.24) $e_R(t) = \cos\left\{\omega_{\text{mod}} \cdot t - (2\pi) \cdot \left[D_{ij}^0 + f_v \cdot (t - t^0) + h_a \cdot (t - t^0)^2\right]\right\}$.

This signal is down-converted by mixing with a local oscillator signal

(A.25) $e_{LO}(t) = \cos\left[(\omega_{\text{mod}} + \omega_{IF}) \cdot t\right]$ to an intermediate frequency signal

(A.26) $E_R(t) = \cos(2\pi) \cdot \left\{ f_{IF} \cdot t + \left[D_{ij}^0 + f_v \cdot (t - t^0) + h_a \cdot (t - t^0)^2\right]\right\}.$

$$= \cos(2\pi) \cdot \{ f_{IF} \cdot t + 2\pi - \Phi_{ij}(t)\} \quad (0 < \Phi_{ij}(t) < 2\pi).$$

The mean phase shift of the down-converted received signal relative to the intermediate frequency oscillator signal $\cos(\omega_{IF} \cdot t)$, averaged over the integration time interval is:

(A.27) $(\overline{\Delta\Phi})_{ij} = 2\pi - \left(\frac{2\pi}{\Delta t_i}\right) \cdot \int_{t^0 - \Delta t_i/2}^{t^0 + \Delta t_i/2} \left[D_{ij}^0 + f_v \cdot (t - t^0) + (\frac{\eta \cdot a_0}{\lambda_m}) \cdot (t - t^0)^2\right] dt$

This gives, independent of the range Doppler rate f_v,

(A.28) $$(\overline{\Delta\Phi})_{ij} = 2\pi - (2\pi) \cdot \left[D_{ij}^0 + \frac{1}{24} \cdot \frac{\eta \cdot a_0 \cdot (\Delta t_i)^2}{(\lambda_m/2)}\right].$$

If one interprets the mean phase delay over the integration time interval as being due to an effective measured normalized optical path length, this is the path at mid-interval plus an acceleration-generated path term, the last term in (A.28): one then subtracts a contribution $\frac{a_0 \cdot (\Delta t_i)^2}{24}$ from the measured range to obtain the range at mid-interval time t_{ij}^0.

Actually, rangefinder phase processing is done by a digital sampling procedure, described in [Pay-1]. A detailed analysis of that signal-processing procedure, applied to the signal $E_R(t)$, is needed to confirm the use of (A.28) as a range estimator. This is done in appendix H. A small additional correction term: D_{corr} is available to account for range rate effects. One replaces D_{ij}^0 in (A.28) by $D_{ij}^0 - D_{corr}$ where

(A.29) $D_{corr} = (\frac{1}{4\pi}) \cdot (\frac{f_v}{f_{IF}}) \cdot \sin(4\pi \cdot D_{ij}^0) + \sqrt{3} \cdot (\frac{f_v}{f_{IF}})^2 \cdot (1 - \cos(4\pi \cdot D_{ij}^0))$

This term is always negligible, except for the case of rapid tracking scans used

during telescope mapping measurements. In appendices G and H we show that the acceleration term is aways small enough to be neglected.

The angle of illumination incidence was previously assumed to be zero. In all range measurements, the incidence angle is nearly constant during illumination, and one can correct for non-normal incidence by using the static incidence angle correction given by equation (A4.1) of GBT Memo 154 [Gol-2].

If the normal to the entry face of the target prism is at angle of incidence I_{in} to the incoming laser beam, there is an incremental range correction:

$$\text{(A.30)} \quad \Delta R(I_{in}) = \left\{ D\left(n - \sqrt{n^2 - \sin^2(I_{in})}\right) - \left(\frac{D}{n}\right)(1 - \cos(I_{in})) \right\}$$

to be added to the measured range. This differential correction vanishes when $I_{in} = 0$. The correction has a negative value when $I_{in} > 0$. The instrument phase shift, including the case of oblique incidence, is then:

$$\text{(A.31)} \quad (\overline{\Delta\Phi})_{ij} = 2\pi - (2\pi) \cdot \left[D^0_{ij} - D_{corr} + (\frac{\eta}{(\lambda_m/2)}) \cdot (\Delta R(I_{in})) \right].$$

A caution! There is a possibility of occasional cycle jump in measurement. The path phase residual (the right side of (A.31)) will be the measured electronic phase residual only if the (positive) term in brackets is less than 1. If that is not true, electronic phase will jump by $+2\pi$. (Larger jumps are not possible, given the known limits on size of the last two bracketed terms). The last term in brackets is almost always much smaller than the distance residual D^0_{ij}, and typically is smaller than $0.1\,mm$. Its presence will rarely force the bracket term in (A.31) to exceed 1. When that rare event does occur, the measured electronic phase will be too large by 2π. Most generally, we have:

$$\text{(A.31.1)} \qquad (\overline{\Delta\Phi})_{ij} = \left((\overline{\Delta\Phi})_{ij}\right)_{\text{electr}} - (2\pi) \cdot \mathbf{I}_{ij}$$

where $\mathbf{I}_{ij} = 0$ or 1, but is almost always 0.

To eliminate common mode path, the rangefinder measures range along a comparison path. That path runs from the laser diode to the rangefinder scan point to a calibration reference prism, back to the scan point and then to the photodetector surface. The one-way normalized optical length of this internal calibration reference path within the rangefinder is:

$$\text{(A.17.1)} \quad \mathcal{S}_{ii} = \frac{\eta \cdot [(L_{cmm})_i + (L_{spc})_i] + \eta_{glass} \cdot (D)_i}{(\lambda_m/2)} \, .$$

Here $(D)_i$ is the depth of the calibration reference prism reflector on rangefinder ZY_i. The length $(L_{spc})_i$ is the normal distance from the mirror scan point of rangefinder ZY_i to the entry face of the reference prism; this distance is measured with gauge blocks in the laboratory and is included in the rangefinder's data base.

The modular phase shift of the down-converted signal for the calibration path is then:

$$\text{(A.31.1)} \quad (\overline{\Delta\Phi})_{ii} = 2\pi - (2\pi) \cdot \left[D_{cmm} + \frac{\eta \cdot (L_{spc})_i}{(\lambda_m/2)} + \frac{\eta_{glass} \cdot (D)_i}{(\lambda_m/2)} \right] .$$

Again, care is needed. If the above term in brackets exceeds 1, the measured electronic phase will be greater than the path phase on the right side of (A31.1) by 2π, and cycle slip occurs. This possible phase jump in the reference calibration path will either never occur, or will always occur. Its occurrence is a property of the rangefinder geometry. Its presence is determined by measuring a sequence of closely spaced known external range paths in the laboratory. We can write:

$$\text{(A.31.2)} \qquad (\overline{\Delta\Phi})_{ii} = \left((\overline{\Delta\Phi})_{ii} \right)_{\text{electr}} - (2\pi) \cdot \mathbf{I}_{ii} \quad \text{where} \quad \mathbf{I}_{ii} = 0 \text{ or } 1 \, ,$$

and is determined by laboratory measurements. Here,

$$\text{(A.31.3)} \qquad \mathbf{I}_{ii} = \text{Int} \left[D_{cmm} + \frac{\eta \cdot (L_{spc})_i}{(\lambda_m/2)} + \frac{\eta_{glass} \cdot (D)_i}{(\lambda_m/2)} \right] .$$

To remove the common mode path, subtract equation (A.31.1) from (A.31):

$$\text{(A.32)} \quad (\lambda_m/2) \cdot D^0_{ij} = (\lambda_m/2) \cdot \left(\frac{(\overline{\Delta\Phi})_{ii} - (\overline{\Delta\Phi})_{ij}}{2\pi} + (D_{cmm})_i + D_{corr} \right)$$
$$+ \eta \cdot (L_{spc})_i + \eta_{glass} \cdot (D)_i - \eta \cdot \Delta R(I_{in}) \, .$$

Range residual D^0_{ij} is found by first computing the right side of (A.32) assuming that $D_{corr} = 0$, then computing D_{corr} by means of (A.29) using the value just found for D^0_{ij} and, finally, recomputing D^0_{ij} using (A.32) but now including the newly-computed value of D_{corr}.

The distance d_{ij}^0 between the scan point of ZY_i and the reference point of target T_j, at time t^0, is found by substituting the right side of (A.32) into

$$(A.22.2) \qquad d_{ij}^0 = (\frac{1}{\eta}) \cdot \left\{ (\mathcal{N}_{ij} + D_{ij}^0 - (D_{cmm})_i) \cdot (\frac{\lambda_m}{2}) \right\} - |P_c|_j \ .$$

Our final result is:

$$(A.33) \quad d_{ij}^0 = \left(\mathcal{N}_{ij} + \frac{\left((\overline{\Delta\Phi})_{ii}\right)_{\text{electr}} - \left((\overline{\Delta\Phi})_{ij}\right)_{\text{electr}}}{2\pi} + \mathbf{I}_{ij} - \mathbf{I}_{ii} + D_{corr} \right) \cdot (\frac{\lambda_m}{2\eta})$$

$$- |P_c|_j \ - \Delta R(I_{in}) + (L_{spc})_i + n \cdot (D)_i \ .$$

We note that $(D_{cmm})_i$ does not appear explicitly in the final range equation.

In the result above $\mathbf{I}_{ij}$ is 0 or 1, but is almost always 0. It cannot be proved to be zero, without additional information. When electronic phase measurement is modular, there is loss of information. If a sum of individual residual lengths (each less than $\lambda_{\text{mod}}/2$) adds up greater than $\lambda_{\text{mod}}/2$ (in our case $10\,cm$), the modular sum is the physical sum of the lengths decreased by the integer number of half modulation wavelengths contained in that sum. (For commercial rangefinders, ambiguity caused by modular counting is resolved by use of multiple frequencies). For the GBT metrology system, contributions due to incidence angle and acceleration correction terms are small. The common mode path residue is eliminated as a contributor to the residual length sum by the stratagem of: measuring it a-priori in the laboratory, then including its measured value as a contributor to the modular range, it subsequently cancels out when the calibration reference path phase (to which it contributes) is subtracted from the range path phase. For the calibration reference path one obtains the correct electronic phase, as discussed above. But for the range path, it is not usually possible guarantee *a-priori* that no phase jump will occur.

[One may however resolve this ambiguity by use of multiple ranges. In trilateration adjustments of measured distance of a target from four rangefinders, one trilaterates ranges which are reduced assuming that $\mathbf{I}_{ij}$ is zero. The trilateration converges if this is, in fact, the case. If convergence fails, one can replace the

target by a sequence of "pseudotargets", where a pseudotarget's distance to each rangefinder is computed using $\mathbf{I}_{ij} = 0$ or 1 arbitrarily in the range reduction (subject to the condition that $\mathbf{I}_{ij}$=1 for at least one of the reduced ranges) in seven combinations. Exactly one trilateration can converge. The procedure is clumsy, but can be used when all else fails. Another procedure, is to flag and compensate sudden range jumps in a multiple scan range trajectory determination, if the magnitude of the jumps is near $10\,cm$ and one is otherwise confident that the range is known correctly to $5\,cm$.]

If the retroreflector target T_j is a glass corner prism we use

$$(A.34) \qquad |P_c|_j \;=\; +D \cdot (n - \frac{1}{n}) \; .$$

If the target T_j is a ball retroreflector we use

$$(A.34.1) \qquad |P_c| \;=\; n \cdot (R_1 + R_2) - R_1 \; , \quad \text{and} \quad \Delta R(I_{in}) = 0 \; ,$$

where R_1 is the inner ball radius and R_2 is the outer ball radius.

Using design values for the ball retroreflectors: $R_1 = 1.969"$, $R_2 = 3.799"$, group refractive index $\eta_{glass} = 1.527463$ (for BK7 glass) and $\eta = 1.00025324$ for air at $20°C$ temperature, 933 mb pressure, 50% relative humidity; the length correction constant for the design ball reflector is $P_c = -173.715\,\text{mm} = -6.8392"$. $|P_c| \;=\; +173.715\,\text{mm}$. The target reference point for the ball reflector is the common center point of the two ball surfaces.

Equation (A.32) computes range distance between the scan mirror reference point S_i of an illuminating rangefinder and the fiducial reference point T_j of an illuminated retroreflector target. When one measures distance between scan-mirror reference points, S_i and $S_{i'}$, of two rangefinders (A.32) obviously can not be used. ($S_{i'}$ is not a fiducial reference point of a retroreflector target). However one can compute distance between two scan-mirror points using a modified calculation. (When calculating such distance in the ZY_i-computer, one provides a flag to signal the special case of measurement between rangefinder scan mirror reference points). This will always be a static measurement, or one in which range rate corrections are unnecessary. The modified calculation follows.

The actual distance measurement is between S_i and the fiducial point $T_{i'}$ of the prism retroreflector of the targeted rangefinder in anti-autocollimation. The distance between scan points, $|\, S_i S_{i'} \,|$, is related to the measured distance $|\, S_i T_{i'} \,|$ by equation (2.5.1). We have,

$$|\, S_i T_{i'} \,| = |\, S_i S_{i'} \,| - (H)_{i'} + \frac{(D_{sm})_{i'}}{n} . \tag{A.35}$$

Let us call $d_{S_i S_{i'}}(AZ, EL)$ the current tabulated available distance between the mirror scan reference points. In place of the normalized modular range integer $\mathcal{N}_{ij}$ in equations (A.21) and (A.32) we use a modified normalized modular range integer:

$$\mathcal{N}_{ii'} = \text{Int}\left\{ \frac{\eta \cdot \left[d_{S_i S_{i'}}(AZ, EL) - (H)_{i'} + \dfrac{(D_{sm})_{i'}}{n} + |P_c|_{i'} \right] + (D_{cmm})_i}{(\lambda_m/2)} \right\} . \tag{A.36}$$

Note that the prism depth above is that of the targeted retroreflector prism, on the target rangefinder's scan-mirror, and not the reference path prism of the illuminating rangefinder. Here, we denote the depth of the targeted scan-mirror prism as $(D_{sm})_{i'}$, that of the reference path prism of the target rangefinder by $(D)_{i'}$, and that of the reference path prism of the illuminating rangefinder by $(D)_i$. In the measurement, illumination is normal to the targeted prism, and there is no incidence angle correction.

After measuring the distance $|\, S_i T_{i'} \,|$ one adds back $(H)_{i'} - \dfrac{(D_{sm})_{i'}}{n}$ to give the measured distance between scan-mirror reference points:

$$|\, S_i S_{i'} \,| = \left(\mathcal{N}_{ii'} + \frac{\left((\overline{\Delta\Phi})_{ii}\right)_{\text{electr}} - \left((\overline{\Delta\Phi})_{ii'}\right)_{\text{electr}}}{2\pi} + \mathbf{I}_{ii'} - \mathbf{I}_{ii} \right) \cdot \left(\frac{\lambda_m}{2\eta}\right) \tag{A.37}$$

$$+ \left[(H)_{i'} - \frac{(D_{sm})_{i'}}{n} \right] - |P_c|_{i'} + (L_{spc})_i + n \cdot (D)_i .$$

Appendix B. Time Interpolation And Extrapolation Of Ranges.

We start with a set of $1 + (m_{\max})_{ij}$ measured range distances,

$$(B.1) \qquad d_{ij}(t = t_{ij}(p,m)) \;=\; d_{ij}(t^0_{ij}(p) + m \cdot h) \qquad (\, m = 0,\, \ldots\, , (m_{\max})_{ij}\,)$$

from rangefinder ZY_i to retroreflector target T_j. The measurement time for this set of ranges spans the time interval

$$(B.2) \qquad t^0_{ij}(p) - \frac{\Delta t_i}{2} \;\leq\; t \;\leq\; t^0_{ij}(p) \;+\; h \cdot (m_{\max})_{ij} \;+\; \frac{\Delta t_i}{2}\,.$$

We wish to generate a range, $d_{ij}(t)$, from the measured range data, for arbitrary values of t, together with an estimate of the maximum error, $\mathrm{erest\_}d_{ij}(t)$. When t lies inside the measurement time interval we *interpolate*, when t lies outside that interval we *extrapolate.*

Given a smooth analytic function and a *uniformly spaced* set of tabulated values of the given function, there are several ways to interpolate the the function using finite-difference methods. One can do forward or backward Newtonian interpolation, starting from the first tabulated value and using forward differences or starting from the last tabulated value and using backward differences. One can also interpolate from a tabulated value near the center of the list of tabulated values and use central differences (Bessel interpolation). These methods are described in [Hil-1] and [ESA-1] and error bounds are given for error due to truncation of the interpolating series. We give an example of a Bessel interpolation in Appendix D.

Telescope retroreflector motion is smooth in this sense, and consists of the driven motion together with vibratory motion. But the rangefinder measurements have stochastic noise due to short-time refractivity fluctuations and electronic phase noise. One then faces the question: should one perform range interpolation)or extrapolation) using tabulated sets of measured ranges or should one perform digital smoothing or filtering on the measured range data set before interpolating.

That is, the measured range set is obtained in an environment of: telescope motion, vibration, wind gust loading and atmospheric refraction and electronic phase noise. Under such conditions one might wish not merely to perform math-

ematical extrapolation or interpolation, but also to do digital filtering of the data set or use a predictive statistical estimator approach, for example Kalman filtering. A large literature exists on these methods [IEEE-1]. Commercial and non-commercial software is available.

One may wish to use time-extrapolations of ranges in two different ways. In the Phase III of telescope operations, it might be desirable to do short term extrapolation of dynamical range trajectories, to provide predictive pointing correction estimates for the immediate future (expected current trajectory future values minus commanded values) to generate elevation and azimuth angle dynamical pointing corrections for monitor and control of the telescope. One might also wish to do *a-postiori* fitting of target range trajectories, to generate optimal measured values of pointing angles, for data archives of the telescope observing run.

It may happen, for some scan scenarios, that the scan measurements to a target retroreflector can not be made at uniformly spaced time intervals. Under those conditions finite-difference interpolation methods are inappropriate. In such cases, one uses other algorithmic methods.

Source code routines for Neville type algorithms, useful for computing tabular data extrapolations, are given in [Pre-1], in C-language. From arrays of data $t^0_{ij}[0, 1, \ldots, (m_{\max})_{ij}]$ and $d^0_{ij}[0, 1, \ldots, (m_{\max})_{ij}]$ and given a value t the extrapolation routine returns a value $d_{ij}(t)$ and an error estimate $\mathrm{erest}\_d_{ij}(t)$.

The routines given in [Pre-1] are available for both polynomial and rational function approximations. The extrapolation polynomial or rational function is not generated explicitly in the computation; only the extrapolated range and error estimate are returned. The routines are given in Appendix E.

We note that before using these routines the measured ranges are corrected for cycle slip phase jumps.

Appendix C. Extrapolated Trilaterations.

To start, we assume that we are given sets of range distances

(C.1) $d_{ij}(t = t_{ij}(p,m)) = d_{ij}(t^0_{ij}(p) + m \cdot h) \qquad (\, m = 0, \ldots, (m_{\max})_{ij}\,)$

measured from rangefinder ZY_i to retroreflector target T_j.

Here h is the inner scan loop cycle time (Fig. 4), $h = \Delta t_{cyt}$, and

(C.2) $\qquad t^0_{ij}(p) = t^0 + p \cdot \Delta t_{cy} + t^{00}_{ij}$

where t^0 is a scan scenario reference start time, p is the number of complete outer scan loop cycles completed, and t^{00}_{ij} is the mid-scan offset delay time of scan $m = 0$ of range pair S_iT_j from the start of the previous outer scan loop.

The first inner scan loop measurement is made at mid-scan time $t^0_{ij}(0)$. An additional measurement is made every h seconds, until $(1+(m_{\max})_{ij})$ measurements have been completed. Here, $h = \mathcal{H} \cdot \tau$, where $\tau = 1$ millisecond and $\mathcal{H}$ is an integer. The times t for our common clock timing signal are an integer number of milliseconds. The interval h between successive scans of our rangefinder-target pair is, then, an integer multiple of 1 millisecond. For all scan times and all range pairs, the difference of any two of these times is an integer multiple of one millisecond. The clock timing signals are provided to the metrology system computers in IRIG timing format.

That is, scan measurements and interpolations are synchronized with the ticks of a master timer which beats on the second and at 1-millisecond intervals with respect to some time scale. We assume that the range pair S_iT_j makes a sequence of $(1 + (m_{\max})_{ij})$ scans, which start at mid-scan time $t^0_{ij}(p) - \dfrac{\Delta t_i}{2}$ and repeat every h seconds. Each scan requires an integration time Δt_i. The range distance mid-scan measurement times are:

(C.3) $\qquad t_{ij}(p,m) = t^0_{ij}(p) + m \cdot h \qquad (m = 0, \ldots, (m_{\max})_{ij}).$

The master timer for the rangefinder metrology system provides a precise 1-kHz intermediate frequency, so that individual scan integration times are precise integer multiples of one intermediate frequency period. (In fact, the 1 kHz signal is obtained by division of a 64 kHz signal used for 6-bit time sampling of the rangefinder return signal).

To refer the scan times of the several observing rangefinders to a common reference time we have already assumed that

(C.2) $$t^0_{ij}(p) = t^0 + p \cdot \Delta t_{cy} + t^{00}_{ij} \ ,$$

and the scan program involving multiple rangefinders and targets is referred to a common initial time, t^0, for all of the range pairs, and first inner loop scan time offset t^{00}_{ij} for the pair S_iT_j. We also assume now that the times t^0 and t^{00}_{ij} are integer numbers of milliseconds.

We want to extrapolate or interpolate available sets of measured range distances, to generate a range distance $d_{ij}(t = t^0 + \Delta)$ for each rangefinder-target pair, referred to the common time $t = t^0 + \Delta$.

For ground-based scanning rangefinders, scan point locations are fixed and known. For each range pair one can extrapolate the time series of ranges $d_{ij}(p, m)$_measured at mid-scan times

(C.4) $$t_{ij}(p, m) = t^0 + p \cdot \Delta t_{cy} + t^{00}_{ij} + m \cdot h$$

to the extrapolated range $d_{ij}(t^0, \Delta)$ referenced to time $t = t^0 + \Delta$. One then uses the extrapolated ranges together with known ground frame coordinates of the observing rangefinders and the survey standard errors as input data for an extrapolated coordinate determination, referred to the time $t^0 + \Delta$. One can repeat this procedure, choosing different values for Δ to obtain other extrapolated locations on the trajectory. Subsequently one may trilaterate ranges, measured by several rangefinders to a common target and extrapolated to the common time $t^0 + \Delta$, to estimate target coordinates at the time $t^0 + \Delta$. In performing the trilateration estimate one uses as input data survey coordinates and coordinate standard errors of the ground rangefinders together with the set of extrapolated

trajectory ranges and the extrapolation error bounds erext_$d_{ij}(t^0+\Delta)$ as standard errors of the extrapolated range measurements.

For each range measurement program involving dynamic range measurement followed by extrapolated trilateration and trajectory estimation or prediction, detailed computer code modules will have to be developed for control of the the rangefinder measurements and processing of data.

There is an important systems consideration which requires investigation. This is the question of error handling associated with range adjustment and coordinate determination. In the case that the range adjustment procedure fails to converge, for any reason, an error flag must be generated and an error-handling-command signal must be sent to each potential recipient of the adjustment data. The nature of the error handling commands will depend upon which of the range scan programs is in progress.

Appendix D. Bessel Interpolation.

Let s be a real variable and let

(D.1) $t = t^0 + s \cdot h$.

A finite-difference degree-4 Bessel polynomial interpolation using five uniformly spaced tabulated values of a function $f(t)$, is given in [ESA-1]. Using the definition of the central difference operator:

(D.2) $\delta f(t^0 + mh) = f(t^0 + mh + \frac{h}{2}) - f(t^0 + mh + \frac{h}{2})$,

Bessel's interpolation formula is, in the notation of Table I :

(D.3) $f(t) = f(t^0) + s \cdot \delta_{1/2} + B_2(\delta_0^2 + \delta_1^2) + B_3\delta_{1/2}^3 + B_4(\delta_0^4 + \delta_1^4) + \cdots$, where

(D.4) $B_2 = s \cdot (s-1) \cdot \left(\frac{1}{4}\right)$,

(D.5) $B_3 = s \cdot (s-1) \cdot (s - \frac{1}{2}) \cdot \left(\frac{1}{6}\right)$,

(D.6) $B_4 = (s+1) \cdot s \cdot (s-1) \cdot (s-2) \cdot \left(\frac{1}{48}\right)$. and

(D.7) $\delta_{1/2} = f_1 - f_0 = f(t^0 + h) - f(t^0 - h)$,

(D.8) $\delta_0^2 = f_1 - 2 \cdot f_0 + f_{-1}$, , $\delta_1^2 = f_2 - 2 \cdot f_1 + f_0$,

(D.9) $\delta_0^2 + \delta_1^2 = f(t^0 + 2h) - f(t^0 + h) - f(t^0) + f(t^0 - h)$,

(D.10) $\delta_{1/2} = f_1 - f_0 = f(t^0 + h) - f(t^0)$.

(D.11) $\delta_{1/2}^3 = \delta_1^2 - \delta_0^2 = f(t^0 + 2h) - 3 \cdot f(t^0 + h) + 3 \cdot f(t^0) - f(t^0 - h)$.

(D.12) $\delta_0^4 + \delta_1^4 = f(t^0 + 2h) - 4 \cdot f(t^0 + h) + 6 \cdot f(t^0) - 4 \cdot f(t^0 - h) + f(t^0 - 2h)$.

A full series expansion in s appears in [Hil-1], with a truncation error bound.

Appendix E. Polynomial And Rational Function Extrapolation.

Here we present polynomial and diagonal rational function approximations to compute extrapolated or interpolated range.

Arrays of measured range data are given:

$$\text{tij}[1], \ldots, \text{tij}[N] \quad \text{and} \quad \text{dij}[1], \ldots, \text{dij}[N] \quad \text{and a time} \quad t\,.$$

The data value dij[m] is a measured range from rangefinder i to target j at mid-scan time tij[m], where m is an integer ($0 \leq m \leq N$). The time t is a value of time to which the measured range data is extrapolated or interpolated, to generate a corresponding (extrapolated or interpolated) range value: dist . The measurement times, tij[m], do not have to be uniformly spaced.

The routines which follow are in C^{++}-language, and were adopted from Chapter 3 of "*Numerical Recipes In C*" [Pre-1]. Some changes of notation were made. The routines use Neville type algorithms to perform the numerical computations. The theory of the method is given in [Pre-1].

A header file "util.h" is used to define vectors and error handling. Vectors are floating point in the routines; modified declarations, indicated in the header file can be made, to employ double precision. To do that, vectors in the given interpolation routines are replaced by double precision vectors.

```
//*******  Header file  util.h  **********

include <stdio.h>
include <math.h>
include <malloc.h> //Needed for some compilers.

void  runerror(error_text);
char  error_text[];  //Standard error handler.
  {
   void  exit();
   fprintf(stderr, Run-time Error! \n");
   fprintf(stderr, %s\n" , error_text) ;
   fprintf(stderr, "Now Exiting To System! \n") ;
   exit(1) ;
  }
```

```
float *vector(nl,nh); //Allocate float vector, range [nl...nh].
int   nl, nh;
  {
   float  *v ;

   v=(float *)malloc((unsigned) (nh-nl+1)*sizeof(float)) ;
   if  (!v)  runerror(Allocation failure in vector()")   ;
   return  v-nl  ;
  }

double *dvector(nl,nh) //Allocate vector, range [nl..nh]
int   nl, nh ;
  {
   double  *v ;

   v=(double *)malloc((unsigned) (nh-nl+1)*sizeof(float)) ;
   if  (!v)  runerror(Allocation failure in vector()")   ;
   return  v-nl  ;
  }

void  free_vector(v,nl,nh)
float    *v      ;
int      nl, nh  ;
   // Frees a float vector allocated by vector().

  {
    free((char*) (v+nl)) ;
  }

void  free_dvector(v,nl,nh)
double *v     ;
int    nl, nh ;
  // Frees vector allocated by vector().

  {
    free((char*) (v+nl)) ;
  }
```

```
//*********** Polynomial interpolation routine polyint()  **********


//  Given arrays tij[1],..., tij[N] and dij[1],..., dij[N] and
//  time t this routine returns a value dist and error estimate
//  erest_d. If P(t) is the polynomial of degree N-1  such that
//  P(tij[n]) = dij[N] for (n=1, ... , N), then the returned
//  value for P(t) = dist.

#include  <util.h>

void    polyint(tij, dij, N, t, dist, erest_d) ;
float   tij[], dij[], t, *dist, *erest_d ;
int     N ;
  {
        int     i, m, ns=1;
        float   den, dif, dift, ho, hp, w ;
        float   *c, *d, *vector() ;
        void    runerror(), free_vector() ;

        dif = fabs(t-tij[1]) ;
        c = vector(1,N)      ;
        d = vector(1,N)      ;

        for  (i=1 ; i<=N ; i++) {
          // Find index ns for closest table entry.

            if ((dift=fabs(dist-dij[i])) < dif )  {
                ns=i     ;
                dif=dift ;
            }
            c[i]=tij[i] ;   //Initialize c[], d[] lists.
            d[i]=dij[i] ;
        }

        *dist=dij[ns--] ;  //Initial approximation to dist.

          // For each list column, loop over the
          // current c's and d's, and update them.
```

```
        for (m=1; m<N; m++) {
          for (i=1; i<=N-m; i++) {
           ho=tij[i]-t   ;
           hp=tij[i+m]-t ;
           w=c[i+1]-d[i] ;
           if ((den=ho-hp)==0.0) runerror("Error in POLYINT routine.");
             // This occurs only if two dij[] coincide.
           den=w/den     ;
           d[i]=hp*den   ;  //Update c's and d's
           c[i]=ho*den   ;
          }

          *dist += (*erest_d=(2*ns < (N-m) ? c[ns+1] : d[ns--]));
        }
        free_vector(d, 1, N)  ;
        free_vector(c, 1, N)  ;
}
```

```
//****** Rational function routine  ratintp()  ********


#include <math.h>

#define  TINY  1.0e-25
#define FREERETURN  {free_vector(d,1,N) ; free_vector(c,1,N) ; return};

void    ratintp(tij, dij, N, t, dist, erest_d) ;
float   tij[], dij[], t , *dist, *erest_d ;
int     N ;

//  Given arrays  tij[1],..., tij[N] and dij[1],..., dij[N] and
//  time t this routine returns a value dist and error estimate
//  erest_d.  The value returned is that of the diagonal rational
//  function evaluated at t which passes through the points
//  (tij[m], dij[m]), m=1...N.

{
    int    m, i, ns=1 ;
    float  w, tt, hh, h, dd, *c, *d *vector() ;
    void   runerror(), free_vector() ;

    c=vector(1, N) ;
    d=vector(1, N) ;
    hh=fabs(t-tij[1]) ;
    for  (i=1, i<=N; i++)  {
        h=fabs(t-tij[i]) ;
        if  (h == 0.0)  {
            *dist=dij[i] ;
            *erest_d=0.0 ;
            FREERETURN
        }  else if (h < hh)  {
            ns=I ;
            hh=h ;
        }
        c[i]=dij[i] ;
        d[i]=dij[i]+TINY ;  //Increment needed to avoid 0/0.
    }
```

```
    *dist=dij[ns--] ;

    for  (m=i; m<N; m++)  {
        w=c[i+1]-d[i] ;
        h=tij[i+m]-t  ;
        tt=(tij[i]-t)*d[i]/h ;
        dd=tt-c[i+1] ;

        if  (dd == 0.0) runerr("Error in routine RATINTP") ;
           // Announces pole at requested value of t.
        dd=w/dd ;
        d[i]=c[i+1]*dd ;
        c[i]=tt*dd ;
     }
     *dist += ((*erest_d=(2*ns < (N-m) ? c[ns+1] : d[ns--])) ;
   }
   FREERETURN
}
```

Appendix F. Symbol List .

t	Time variable
P	Target or rangefinder fiducial reference point
$\overrightarrow{r}(P;t)$	Displacement of P from ground frame origin
$P(t)$	General reference to location of fiducial
	point P as a function of time
T_j	Fiducial reference point of retrotarget "T_j"
S_i	Scan reference point of rangefinder ZY_i
$EL(t)$, $AZ(t)$	Generic elevation, azimuth, at time t
$EL_{enc}(t)$, $AZ_{enc}(t)$	Encoder readout angle output at time t
$EL_{com}(t)$, $AZ_{com}(t)$	Commanded encoder angles for time t
$X(P;t), Y(P;t), Z(P;t)$	Ground frame coordinates of P at time t
$X_{rg}(P), Y_{rg}(P), Z_{rg}(P)$	Geometric reflector frame coordinates of P
$X_r(P;EL)$, $Y_r(P;EL)$,	Reflector frame coordinates of P computed
$Z_r(P;EL)$	from Finite Element Model
$d(S_i,T_j;t) = d_{ij}(t)$	Distance from scan point S_i to target T_j

$\overrightarrow{r}_{ij}(S_i, T_j; t_{ij})$	Displacement of T_j from S_i at time t_{ij}
$d_{ij}(S_i, T_j; t_{ij})$	Distance from S_i to T_j at time t_{ij}
$d_{ij}(AZ, EL)$	Distance, S_i to T_j, computed from
	current coordinate data and the
	Finite Element Model
$(D)_j$	Depth of target prism .
$(P_c)_j$	Target prism range correction constant.
$(D)_i$	Rangefinder comparison prism depth
$m_{ij}\ (= m)$	Scan sample index for range pair S_i, T_j
$t^0_{ij}(m_{ij})$	Mid-scan time for scan m_{ij} of pair S_i, T_j
$h_{ij} = \Delta t_{cyt}$	Cycle period of scans to pair S_i, T_j
Δt_i	Individual scan integration time
$[R13(t)]$	Coordinate transform rotation matrix,
$= [R13\ (AZ(t), EL(t)]$	elevation frame to ground frame.
$[T13(t)]$	Translation column matrix from
	elevation to ground frame

$\lambda_{\mathbf{mod}}$	Laser modulation wavelength. $\lambda_{\mathbf{mod}} = c/f_{\mathbf{mod}}$
η	Group refractive index of air at 780nm
$\mathcal{N}_{ij}$	Int $\left\{ \dfrac{\eta \cdot \left[d_{ij}(AZ, EL) + \lvert P_c \rvert_j \right] + (D_{cmm})_i}{(\lambda_{\mathbf{mod}}/2)} \right\}$
$f(t)$	Smooth real function of time
h	Interpolation interval
t^0	Initial time for scan scenario
s	Interpolating factor. $s = (t - t^0)/h$
$f_m(t)$	$f_m(t) = f(t^0 + mh) \qquad (= f_m)$
δ	Central difference operator
$\delta f_m = \delta_m$	$\delta f_m = f(t^0 + mh + h/2) - f(t^0 + mh - h/2)$
δ_m^2	$\delta_m^2 = \delta_{m+1/2} - \delta_{m-1/2}$
$\delta_{1/2}$	$\delta_{1/2} = f(t^0 + h) - f(t^0) = f_1 - f_0$
δ_0^2	$\delta_0^2 = \delta_{1/2} - \delta_{-1/2} = f_1 - 2f_0 + f_{-1}$
δ_m^n	$\delta_m^n = \delta_{m+1/2}^{n-1} - \delta_{m-1/2}^{n-1}$

d_T	Distance of a cube prism's
	reference point to its face plane
τ_g	One-way propagation time of laser
	signal through glass target prism
$d(t)$	One-way propagation distance from
	rangefinder scan point to cube prism
	reference point, corresponding to signal
	received at time t.
d_0	Distance between rangefinder and
	target reference points at mid-time of
	rangefinder scan.
v_0	Radial velocity component of target
	reference point away from rangefinder
	scan point at mid-time of scan.
a_0	Radial acceleration component of target
	reference point away from rangefinder
	scan point at mid-time of scan.
$(\overline{\Delta\Phi})_{ij}$	Reduced phase shift of down-converted
	received range signal.
$(\overline{\Delta\Phi})_{ii}$	Reduced phase shift of down-converted
	comparison path signal.

$[(\Delta\Phi)_{ij}]_{\text{electr}}$	Measured electronic phase, between
	rangefinder ZY_i and retroreflector
	target T_j.
$[(\Delta\Phi)_{ii}]_{\text{electr}}$	Measured electronic phase, along
	calibration reference path of
	rangefinder ZY_i .
$(D_{cmm})_i$	Optical path length residue in
	units of $\left(\frac{\lambda_{\text{mod}}}{2}\right)$, for calibration
	reference path of rangefinder
	ZY_i , determined during
	laboratory calibration of the
	rangefinder.
$\mathbf{I}_{ii}$	Phase jump integer (0 or 1)
	for calibration reference path
	of rangefinder ZY_i .
	$\mathbf{I}_{ii}$ =Int $\left[D_{cmm} + \frac{\eta \cdot (L_{spc})_i}{(\lambda_m/2)} + \frac{\eta_{glass} \cdot (D)_i}{(\lambda_m/2)} \right]$.
$\mathbf{I}_{ij}$	Phase jump integer (0 or 1) for
	ranging between ZY_i and retroreflector
	target T_j. (Almost always zero).
$(D_{sm})_{i'}$	Depth of scan-mirror retroreflector
	prism of rangefinder ZY_i .

Appendix G. Comments On The Acceleration Correction, Cycle Slip, And Sign Of The Electronic Phase.

Measured range distance, referenced to the center time, t^0, of the range integration time interval $t^0 - \frac{\Delta t_i}{2} \rightarrow t^0 + \frac{\Delta t_i}{2}$ requires a correction to take account of the second time derivative of slant range between rangefinder scan point S_i and target reference point T_j, during the integration time. Under expected scan conditions this derivative can be considered constant during a target scan. Here we discuss the magnitude of the correction.

The distance to be added to correct measured range is: $\frac{(-a_0) \cdot (\Delta t_i)^2}{24}$,

where $a_0 = \frac{d^2}{dt^2} \left(d_{ij}(AZ, EL)\right)_{t=t^0}$.

We tabulate this correction for several values of a_0 and Δt_i:

a_0						
	16	32	64	128	256	Δt_i (millisecond)
$\frac{\text{mm}}{(\text{sec})^2}$						
200	-2.1	-8.5	-34.1	-136.5	-546.1	
100	-1.1	-4.3	-17.1	-68.3	-273.1	
50		-1.3	-8.5	-34.1	-136.5	Distance correction
25		-0.7	-4.3	-17.1	-68.3	(micro-meters)
10			-1.7	-6.8	-27.3	
5			-0.9	-3.4	-13.7	

There are several details to note, concerning this correction. Quantity a_0 is <u>not</u> the acceleration component obtained by projecting the relative acceleration of T_j with respect to S_i onto the line joining these points. It is computed from the range distance function $d_{ij}(AZ, EL)$ using an available model of the telescope geometry, together with the scheduled first and second time derivatives of the telescope azimuth and elevation angles.

A simple example illustrates this. Suppose the telescope to be fixed in elevation and rotating in azimuth at a rate $\frac{dAZ}{dt} = \Omega_{AZ}$. Consider a target point near the center of the main reflector surface, located above the pintle bearing. Suppose a feed arm rangefinder scan point is located at a distance $R \simeq 50$ meters from the pintle bearing. The relative radial acceleration of these points is $R \cdot (\Omega_{AZ})^2$. But their range rate and its time derivative are obviously both zero! In general, the range rate derivative term a_0 is negligible when ranging from a feed arm laser to a surface reflector or a rim prism. It is not intuitively clear whether this is also the case more generally, for example when ranging from the feed arm to a ground benchmark target or from a ground ranger to a rim target ball. Let us next examine such a situation.

Suppose that a feed arm ranger aims to a ground benchmark retroreflector target, while the telescope rotates in azimuth. As a crude model, we assume the rangefinder scan point S_i is at a constant height $S_Z = 90$ meters above the alidade track and has ground coordinates $S_X = R \cdot \cos(\Omega_{AZ} \cdot t)$,
$S_Y = R \cdot \sin(\Omega_{AZ} \cdot t)$. Assume that the target reference point T_j has ground coordinates $T_X = 120$ meter, $T_Y = 0$ meter.

The range between scan and target points swings periodically between a minimum distance

$(d_{ij})_{\min} = \sqrt{90^2 + 0^2 + (120 - 50)^2}$ meters $\simeq 114$ meters and maximum distance

$(d_{ij})_{\max} = \sqrt{90^2 + 0^2 + (120 + 50)^2}$ meters $\simeq 192$ meters.

The range distance in meters versus time is approximately simple harmonic motion:

$$d_{ij}(t) \simeq \frac{(192 + 114)}{2} + \frac{(192 - 114)}{2} \cdot \cos(\Omega_{AZ} \cdot t) = 153 + 39 \cdot \cos(\Omega_{AZ} \cdot t) \ ,$$

with amplitude 39 meters, frequency $\frac{\Omega_{AZ}}{2\pi}$, and $\max \left| \frac{d^2(d_{ij})}{dt^2} \right| \simeq 39 \cdot (\Omega_{AZ})^2 \ \frac{\text{meters}}{\text{sec}^2}$.

The fastest azimuth slew occurs during fast mapping scans, with azimuth rate $\Omega_{AZ} = 40$ degrees/minute $= \frac{\pi}{270}$ radians/second. For the feed arm scan point and benchmark reflector under discussion we get, for fast azimuth slewing,

$$\text{maximum } |a_0| = \text{maximum } \left|\frac{d^2(d_{ij})}{dt^2}\right| \simeq 39000 \cdot (\frac{\pi}{270})^2 \frac{\text{mm}}{\text{sec}^2} = 5.28 \frac{\text{mm}}{\text{sec}^2}.$$

If we assume the same fast slew in elevation, occurring simultaneously, we get for the compound motion, maximum $|a_0| = 5.28\sqrt{2}\,\frac{\text{mm}}{\text{sec}^2}$. For dynamic scans, we will always use $\Delta t_i \leq 0.064$ second. This gives

$$\max \frac{|a_0| \cdot (\Delta t_i)^2}{24} \leq 1.27\ \mu\,\text{meter}.$$

This leads us to conclude that the acceleration correction term can be ignored, under any expected telescope operating conditions!

We now address the question of electronic phase cycle slip during a dynamical scan. We again assume the worst case of simultaneous azimuth and elevation slew of 40 degrees/minute. The maximum range rate between our ranger and benchmark target points occurs when the rangefinder and target are about 1/4 rotation apart in azimuth. The maximum range rate will be

$$\max \left|\frac{d(d_{ij})}{dt}\right| \simeq 39000 \cdot (\frac{\pi}{270}) \frac{\text{mm}}{\text{sec}} = 453.8 \frac{\text{mm}}{\text{sec}}.$$

For a scan lasting $\Delta t_i = 0.064$ second this allows a possible range increment as large as 29 mm during the scan, in the worst case. The probability of a cycle slip is not small for so great a range increment.

This suggests that a range determination should consist of repeated short integration time illuminations, of length a few milliseconds, during dynamical feed-arm-to ground or ground-to-feed-arm scans. That is, one does range trajectory tracking of repeated short individual scans. That procedure will increase the electronic phase noise of the individual scans, while providing more range scan trajectory points. For such a multiple-short-scan time-series scenario one can do a moving digital average of the raw range path electronic phase, and increment the modular range distance $\mathcal{N}_{ij} \cdot \left(\frac{\lambda_{\text{mod}}}{2}\right)$ by $-\left(\frac{\lambda_{\text{mod}}}{2}\right)$ whenever a phase jump

near (-2π) occurs along a gradually increasing phase trajectory (Fig. 9a). One subsequently computes the range distances and interpolates ranges to the center time of this set of scans. In similar manner, whenever a phase jump near $(+2\pi)$ radians occurs along a gradually decreasing phase trajectory (Fig. 9b), one increments the modular range distance by $\left(\frac{+\lambda_{\text{mod}}}{2}\right)$.

We note that in all of the discussions the range path phase was postulated to be a phase delay which decreases with increasing range path. We assumed that the instrumental phase, that is the electronic phase generated by the rangefinder was also decreasing with increasing range path.

Appendix H. Signal Processing.

In order to compare the phase of the down-converted round trip range path signal to that of the intermediate frequency reference signal, one digitally samples the range path signal n times each cycle, where n is equal to 2 raised to a positive-integer power. The IF reference signal is, at frequency f_{IF} is obtained from a signal at frequency $n \cdot f_{IF}$ by frequency division. The digital sampling is thereby done uniformly n times for each IF cycle. At present $f_{IF} = 1000\,\mathrm{Hz}$ and $n = 64$. The range path signal is sampled for a total of m cycles, where m is an even integer, to provide a total of $m \cdot n$ samples.

Let $\mathbf{j}$ be an integer used to index the range path signal samples. Let $s_{\mathbf{j}}$ be the voltage amplitude of the $\mathbf{j}$'th sample. One computes the electronic phase in the following manner. One first computes the following sums over $m.n$ terms.

$$\text{(H.01)} \qquad A \equiv \sum_{\mathbf{j}=0}^{m\cdot n-1} s_{\mathbf{j}} \cdot \cos\left(\frac{2\pi \cdot \mathbf{j}}{n}\right),$$

$$\text{(H.02)} \qquad B \equiv \sum_{\mathbf{j}=0}^{m\cdot n-1} s_{\mathbf{j}} \cdot \sin\left(\frac{2\pi \cdot \mathbf{j}}{n}\right).$$

One then computes the estimated range path signal first harmonic signal amplitude

$$\text{(H.03)} \qquad \mathrm{Ampl} \equiv \left(\frac{2}{m \cdot n}\right) \cdot \sqrt{A^2 + B^2} \quad \text{and the electronic phase}$$

$$\text{(H.04)} \qquad \Phi_{\mathrm{electr}} \equiv ATAN2\left(\frac{B}{A}\right), \quad (0 \le \Phi_{\mathrm{electr}} < 2\pi).$$

The integration time is then $\Delta t_i = m \cdot \left(\frac{1}{f_{IF}}\right)$ and the sampling time is $\tau = \left(\frac{1}{n \cdot f_{IF}}\right)$.

Let us suppose that the intermediate frequency reference signal is

(H.05) $$E_{IF}(t) = \cos(2\pi \cdot f_{IF} \cdot t) ,$$

and the range path return signal is

(H.06) $$E_{Range}(t) = \cos(2\pi) \cdot \left\{ f_{IF} \cdot t + D_{ij}^0 + f_v \cdot (t - t^0) + \left(\frac{\eta \cdot a_0}{\lambda_m}\right) \cdot (t - t^0)^2 \right\} .$$

where $f_v = \dfrac{2 \cdot \eta \cdot v_0}{\lambda_m}$ and D_{ij}^0 is a range residual in units of $\lambda_m/2 \quad (0 \leq D_{ij}^0 < 1)$.

Let $t(\mathbf{j})$ be the time of acquisition of signal sample $s_{\mathbf{j}}$.

The signal is sampled from time $t = t^0 - \dfrac{\Delta t_i}{2}$ to time $t = t^0 - \dfrac{\Delta t_i}{2}$.
We then have:

(H.07) $$t(\mathbf{j} = 0) = t^0 - \left(\frac{m}{2 \cdot f_{IF}}\right) ,$$

(H.08) $$t(\mathbf{j}) = t^0 - \left(\frac{m}{2 \cdot f_{IF}}\right) + \left(\frac{\mathbf{j}}{n \cdot f_{IF}}\right) ,$$

(H.09) $$t(\mathbf{j} = m \cdot n - 1) = t^0 + \left(\frac{m}{2 \cdot f_{IF}}\right) - \left(\frac{1}{n \cdot f_{IF}}\right) .$$

In general, we can assume that t^0 is an integer multiple, I, of $\dfrac{1}{f_{IF}}$ so that

$\cos(\vartheta + (2\pi \cdot f_{IF} \cdot t^0)) = \cos(\theta + (2\pi \cdot I)) = \cos\theta.$

We also note that

$\cos(\vartheta - (2\pi \cdot \dfrac{m}{2})) = \cos(\theta).$

The sampled range path signal values are:

(H.10) $$s_{\mathbf{j}} = E_{range}(t = t^0 - \frac{m}{2 \cdot f_{IF}} + \frac{\mathbf{j}}{n \cdot f_{IF}}) .$$

We also have,

$$(H.11) \qquad t(\mathbf{j}) - t^0 = \left(\frac{1}{f_{IF}}\right) \cdot \left(\frac{\mathbf{j}}{n} - \frac{m}{2}\right) .$$

Substituting, the sampled signal values are then

$$(H.12) \qquad s_{\mathbf{j}} = \cos(2\pi) \cdot \left(\begin{array}{c} f_{IF} \cdot t^0 + \left(\frac{\mathbf{j}}{n} - \frac{m}{2}\right) \cdot \left(1 + \frac{f_v}{f_{IF}}\right) + D_{ij}^0 \\ + \left(\frac{\eta \cdot a_0}{\lambda_m \cdot f_{IF}^2}\right) \cdot \left(\frac{\mathbf{j}}{n} - \frac{m}{2}\right)^2 \end{array} \right) ,$$

which gives, using the periodicity properties above,

$$(H.13) \qquad s_{\mathbf{j}} = \cos(2\pi) \cdot \left(\begin{array}{c} \left(\frac{\mathbf{j}}{n}\right) \cdot \left(1 + \frac{f_v}{f_{IF}}\right) - \frac{m}{2} \cdot \left(\frac{f_v}{f_{IF}}\right) + D_{ij}^0 \\ + \left(\frac{\eta \cdot a_0}{\lambda_m \cdot f_{IF}^2}\right) \cdot \left(\frac{\mathbf{j}}{n} - \frac{m}{2}\right)^2 \end{array} \right) .$$

The signal samples $s_{\mathbf{j}}$ appearing in equation (H.13) may be substituted into equations (H.01), (H.03), (H.04) and the electronic phase shift calculated numerically, for assumed values of the normalized range rate f_v and the second time derivative of range a_0 at the mid-scan time t^0.

The maximum range rate and range acceleration magnitudes expected during GBT operation are $v_0 \simeq 45$ cm/sec and $a_0 \simeq 0.75$ cm/sec^2. For $\lambda_m \simeq 10$ cm and $f_{IF} = 1000$ Hz, we get $|f_v| \leq 4.5$ Hz , $\left|\frac{f_v}{f_{IF}}\right| \leq 0.0045$, $\left|\frac{\eta \cdot a_0}{\lambda_m \cdot f_{IF}^2}\right| \leq 7.5 \times 10^{-8}$.

Numerical computations were run, using the commercially available code "MATHCAD". The effects of varying the parameters: D_{ij}^0, f_v, a_0, Δt_i on the value of the electronic phase Φ_{electr} were investigated.

The following results were obtained, when the range derivatives were within the bounds given above.

1. For a stationary telescope ($v_0,\ a_0,\ f_v = 0$), the formulas (H.01), (H.02), (H.04) accurately give

$$(\text{H.14}) \qquad 1 + (\frac{-1}{2\pi}) \cdot \Phi_{\text{electr}} = D^0_{ij} . \qquad (0 \leq \Phi_{\text{electr}} < 2\pi)$$

2. For a constant range rate ($a_0 = 0$), formulas (H.01), (H.02), (H.04) give

$$(\text{H.15}) \quad 1 + (\frac{-1}{2\pi}) \cdot \Phi_{\text{electr}} + D_{\text{corr}} + \delta = D^0_{ij}$$

where D_{corr} is a small correction which is independent of integration time

and $|\delta| < 2 \times 10^{-6}$.

3. The correction term may be expressed as

$$(\text{H.16}) \qquad D_{\text{corr}} = (\frac{f_v}{4\pi \cdot f_{IF}}) \cdot \sin(4\pi \cdot D^0_{ij}) + \sqrt{3} \cdot (\frac{f_v}{f_{IF}})^2 \cdot (1 - \cos(4\pi \cdot D^0_{ij})) .$$

The remaining range residual error, after making the correction (H.16), is less than 0.2 μm.

4. For the case $f_v = 0\,,\ a_0 \neq 0$,

$$(\text{H.17}) \qquad \left| 1 - \frac{\Phi_{\text{electr}}}{2\pi} + \left(D^0_{ij} + \frac{1}{24} \cdot \frac{\eta \cdot a_0 \cdot (\Delta t_i)^2}{(\lambda_m/2)} \right) \right| < 10^{-7} .$$

CALCULATION OF PHASE SHIFT FOR RANGEFINDER:

Assume n (=64) = samples per cycle,
m = number of cycles in integration time,
f = IF frequency in Hz (= 1000 Hz),
fv = range rate frequency in Hz (= 4.5 for fast scan),
g = fv / f (= 0.0045 for fast scan),
j = sample index (from 0 through m.n-1),
Delta Ti = integration time = m / f (m=32 <=> 32 milliseconds for f = 1000 Hz),
A = cosine-weighted sample sum,
B = sine-weighted sample sum,
D = Range residual distance (0 < D < 1) ,
PHI = Computed Phase (0 < PHI < 360 Degrees).

$$D := 0.025, 0.050 .. 0.975$$

$$n := 64$$

$$g := 0.0$$

$$m := 32$$

$$jmax := m \cdot n - 1$$

$$j := 0, 1 .. jmax$$

$$C(j) := \cos\left(2 \cdot \pi \cdot \frac{j}{n}\right)$$

$$S(j) := \sin\left(2 \cdot \pi \cdot \frac{j}{n}\right)$$

[Omit range acceleration terms]

$$Sig(j) := \cos\left[(2 \cdot \pi) \cdot \left[\frac{j}{n} \cdot (1 + g) + D - m \cdot \frac{g}{2}\right]\right]$$

$$A(D) := \sum_{j} (0 \le j) \cdot (j \le jmax) \cdot C(j) \cdot Sig(j)$$

$$B(D) := \sum_{j} (0 \le j) \cdot (j \le jmax) \cdot S(j) \cdot Sig(j)$$

[Arc-tangent function of B(D)/A(D) , converted to degrees.]

$$PHI(D) := \left(\frac{360.0}{2 \cdot \pi}\right) \cdot angle(A(D), B(D))$$

This run is a computation for a stationary telescope. The range rate and its time derivative are both assumed to be zero.

To make interpretation of the results more transparent, radian quantities have been converted to degrees.

Results for a stationary telescope:

PHI(D)	D·360	360 + (-1)·PHI(D)
351	9	9
342	18	18
333	27	27
324	36	36
315	45	45
306	54	54
297	63	63
288	72	72
279	81	81
270	90	90
261	99	99
252	108	108
243	117	117
234	126	126
225	135	135
216	144	144
207	153	153
198	162	162
189	171	171
180	180	180
171	189	189
162	198	198
153	207	207
144	216	216
135	225	225
126	234	234
117	243	243
108	252	252
99	261	261
90	270	270
81	279	279
72	288	288
63	297	297
54	306	306
45	315	315
36	324	324
27	333	333
18	342	342
9	351	351

CALCULATION OF PHASE SHIFT FOR RANGEFINDER:

Assume n (=64) = samples per cycle,
m = number of cycles in integration time,
f = IF frequency in Hz (= 1000 Hz), (IF frequency)
fv = range rate frequency in Hz (= 4.5 for fast scan),
g = fv / f (= 0.0045 for fast scan),
j = sample index (from 0 through m.n-1),
Delta Ti = integration time = m / f (m=16 <=> 16 milliseconds for f = 1000 Hz),
A = cosine-weighted sample sum,
B = sine-weighted sample sum,
D = Range residual distance (0 <= D < 1) ,
PHI = Computed Phase (0 < PHI < 360 Degrees).

$D := 0.025, 0.050 .. 0.975$

$n := 64$

$g := 0.0045$

$m := 16$

$jmax := m \cdot n - 1$

$j := 0, 1 .. jmax$

$C(j) := \cos\left(2 \cdot \pi \cdot \frac{j}{n}\right)$

$S(j) := \sin\left(2 \cdot \pi \cdot \frac{j}{n}\right)$ [Omit range acceleration terms]

$Sig(j) := \cos\left[(2 \cdot \pi) \cdot \left[\frac{j}{n} \cdot (1 + g) + D - m \cdot \frac{g}{2}\right]\right]$

$A(D) := \sum_{j} (0 \le j) \cdot (j \le jmax) \cdot C(j) \cdot Sig(j)$

$B(D) := \sum_{j} (0 \le j) \cdot (j \le jmax) \cdot S(j) \cdot Sig(j)$

[Arc-tangent function of B(D)/A(D) , converted to degrees.]

$PHI(D) := \left(\frac{360.0}{2 \cdot \pi}\right) \cdot angle(A(D), B(D))$

$RangeErr(D) := (360 \cdot D - (360 - PHI(D))) \cdot \left(\frac{10^5}{360}\right)$

Range path phase, PHI(D), is computed above for the case of a non-zero range rate. Range error is calculated assuming that the modular complement, 1-D, of the mid-scan modular range residual D is directly proportional to range path phase, and one cycle, corresponds to the 10 cm modulation half-wavelength. The range error in micro-meters is given by the variable: RangeErr(D), above.

360 – PHI(D)	D·360	360·D – (360 – PHI(D))
8.9598495	9	0.0401505
17.9223732	18	0.0776268
26.8912209	27	0.1087791
35.869437	36	0.130563
44.8591644	45	0.1408356
53.8614307	54	0.1385693
62.8760392	63	0.1239608
71.901579	72	0.098421
80.9355549	81	0.0644451
89.9746307	90	0.0253693
99.0149591	99	-0.0149591
108.052567	108	-0.052567
117.0837543	117	-0.0837543
126.1054634	126	-0.1054634
135.1155798	135	-0.1155798
144.1131358	144	-0.1131358
153.0983956	153	-0.0983956
162.0728208	162	-0.0728208
171.0389197	171	-0.0389197
180	180	$5.6843419 \cdot 10^{-14}$
188.9598495	189	0.0401505
197.9223732	198	0.0776268
206.8912209	207	0.1087791
215.869437	216	0.130563
224.8591644	225	0.1408356
233.8614307	234	0.1385693
242.8760392	243	0.1239608
251.901579	252	0.098421
260.9355549	261	0.0644451
269.9746307	270	0.0253693
279.0149591	279	-0.0149591
288.052567	288	-0.052567
297.0837543	297	-0.0837543
306.1054634	306	-0.1054634
315.1155798	315	-0.1155798
324.1131358	324	-0.1131358
333.0983956	333	-0.0983956
342.0728208	342	-0.0728208
351.0389197	351	-0.0389197

Range Error (micro-meter) Versus Modular Range Residual

For 45 cm/sec Range Rate, With 1000 Hz IF Frequency.

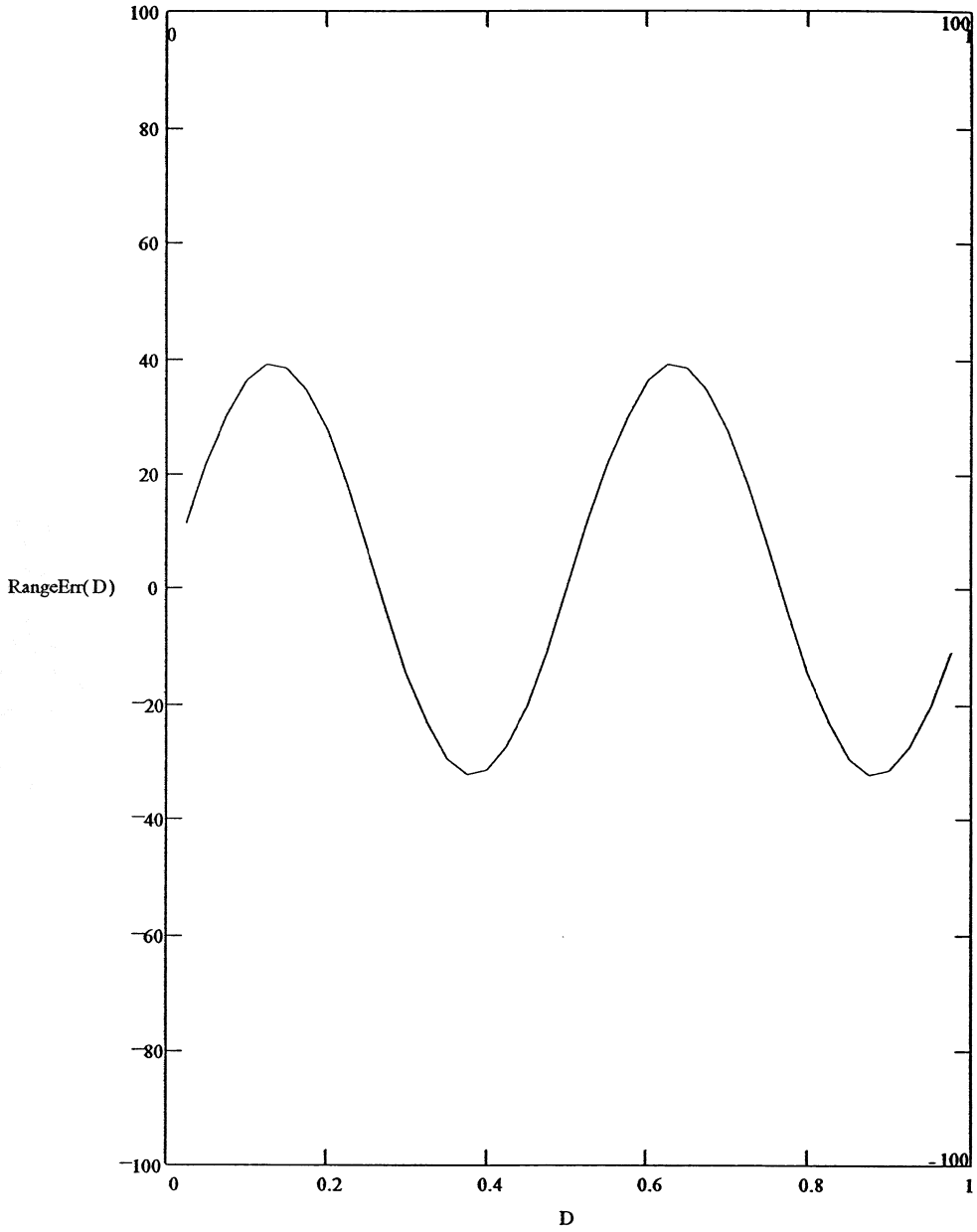

CALCULATION OF PHASE SHIFT FOR RANGEFINDER:

Assume n (=64) = samples per cycle,
m = number of cycles in integration time,
f = IF requency in Hz (= 1000 Hz),
fv = range rate frequency in Hz (= 4.5 for fast scan),
g = fv / f (= 0.0045 for fast scan),
j = sample index (from 0 through m.n-1),
Delta Ti = integration time = m / f (m=32 <=> 32 milliseconds for f = 1000 Hz),
A = cosine-weighted sample sum,
B = sine-weighted sample sum,
D = Range residual distance (0 < D < 1) ,
PHI = Computed Phase (0 < PHI < 360 Degrees).

$$D := 0.025, 0.050 .. 0.975$$

$$n := 64$$

$$g := 0.0045$$

$$m := 32$$

$$jmax := m \cdot n - 1$$

$$j := 0, 1 .. jmax$$

$$C(j) := \cos\left(2 \cdot \pi \cdot \frac{j}{n}\right)$$

$$S(j) := \sin\left(2 \cdot \pi \cdot \frac{j}{n}\right)$$

$$Sig(j) := \cos\left[(2 \cdot \pi) \cdot \left[\left(\frac{j}{n}\right) \cdot (1 + g) + D - m \cdot \frac{g}{2}\right]\right]$$

$$A(D) := \sum_{j} (0 \le j) \cdot (j \le jmax) \cdot C(j) \cdot Sig(j)$$

$$B(D) := \sum_{j} (0 \le j) \cdot (j \le jmax) \cdot S(j) \cdot Sig(j)$$

$$PHI(D) := \left(\frac{180.0}{\pi}\right) \cdot angle(A(D), B(D))$$

Define a correction parameter: Dcorr(D).

$$Dcorr(D) := \frac{g}{4 \cdot \pi} \cdot \sin(4 \cdot \pi \cdot D) + \left(g^2 \cdot \sqrt{3}\right) \cdot (1 - \cos(4 \cdot \pi \cdot D))$$

360 – PHI(D)	D·360	(360 – PHI(D)) + 360·Dcorr(D)
8.9598495	9	9.0003045
17.9223732	18	18.0005593
26.8912209	27	27.0007206
35.869437	36	36.0007678
44.8591644	45	45.0007066
53.8614307	54	54.0005651
62.8760392	63	63.0003825
71.901579	72	72.0001954
80.9355549	81	81.0000273
89.9746307	90	89.999884
99.0149591	99	98.9997573
108.052567	108	107.9996342
117.0837543	117	116.9995079
126.1054634	126	125.9993859
135.1155798	135	134.999291
144.1131358	144	143.9992546
153.0983956	153	152.9993057
162.0728208	162	161.9994577
171.0389197	171	170.9997006
180	180	180
188.9598495	189	189.0003045
197.9223732	198	198.0005593
206.8912209	207	207.0007206
215.869437	216	216.0007678
224.8591644	225	225.0007066
233.8614307	234	234.0005651
242.8760392	243	243.0003825
251.901579	252	252.0001954
260.9355549	261	261.0000273
269.9746307	270	269.999884
279.0149591	279	278.9997573
288.052567	288	287.9996342
297.0837543	297	296.9995079
306.1054634	306	305.9993859
315.1155798	315	314.999291
324.1131358	324	323.9992546
333.0983956	333	332.9993057
342.0728208	342	341.9994577
351.0389197	351	350.9997006

Define:

$$\delta\text{Residual}(D) := D - \left(1 - \frac{\text{PHI}(D)}{360} + \text{Dcorr}(D)\right)$$

Range Error In Micro-Meters Versus Range Residual, D

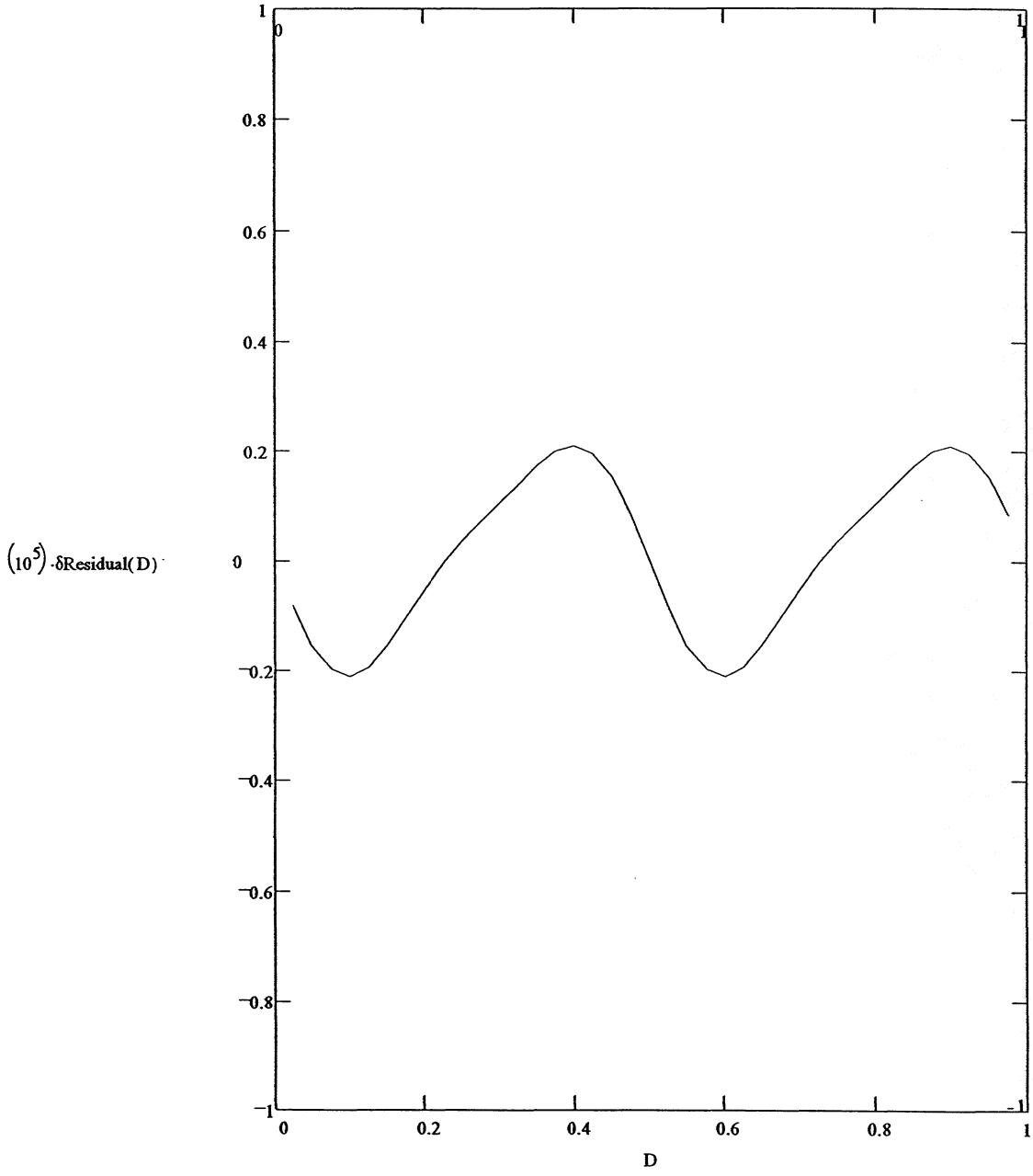

CALCULATION OF PHASE SHIFT FOR RANGEFINDER:

Assume n (=64) = samples per cycle,
m = number of cycles in integration time,
f = IF frequency in Hz (= 1000 Hz),
fv = range rate frequency in Hz (= 4.5 for fast scan),
g = fv / f (= 0.0045 for fast scan),
j = sample index (from 0 through m.n-1),
Delta Ti = integration time = m / f (m=32 <=> 32 milliseconds for f = 1000 Hz),
A = cosine-weighted sample sum,
B = sine-weighted sample sum,
D = Range residual distance (0 < D < 1) ,
PHI = Computed Phase (0 < PHI < 360 Degrees).
ao = second time derivative of range at mid-scan (cm/sec*sec)
nu = group index of air at 780 micro-meters wavelength
lam = modulation wavelength (cm)

$\lambda := 10.0$ $\eta := 1.0$ $ao := 0.75$ $f := 1000.0$

$D := 0.025, 0.050 .. 0.975$

$n := 64$

$g := 0.0000$

$m := 32$

$jmax := m \cdot n - 1$

$j := 0, 1 .. jmax$

$C(j) := \cos\left(2 \cdot \pi \cdot \frac{j}{n}\right)$

$S(j) := \sin\left(2 \cdot \pi \cdot \frac{j}{n}\right)$

$Sig(j) := \cos\left[(2 \cdot \pi) \cdot \left[\left(\frac{j}{n}\right) \cdot (1 + g) + D - m \cdot \frac{g}{2} + h \cdot \left(\frac{j}{n} - \frac{m}{2}\right)^2\right]\right]$

$A(D) := \sum_j (0 \le j) \cdot (j \le jmax) \cdot C(j) \cdot Sig(j)$

$B(D) := \sum_j (0 \le j) \cdot (j \le jmax) \cdot S(j) \cdot Sig(j)$

$PHI(D) := \left(\frac{180.0}{\pi}\right) \cdot angle(A(D), B(D))$

The term ``acc" below is the analytic estimate for range residual shift due to the second time derivative of range:

$h := ao \cdot \frac{\eta}{\lambda \cdot f^2}$

$h = 7.5 \cdot 10^{-8}$

$acc := (2 \cdot h) \cdot \left(\frac{1}{24}\right) \cdot (m)^2$

$acc = 6.4 \cdot 10^{-6}$

The phase computation algorithm above includes both range rate and acceleration terms. The present run is performed assuming non-zero acceleration, but zero range rate at mid-scan. The result is compared to that expected for the analytic approximation which computes phase using the mean range shift due to acceleration averaged over the scan.

360 – PHI(D)	D·360	(D + acc)·360
9.0023037	9	9.002304
18.0023037	18	18.002304
27.0023038	27	27.002304
36.0023039	36	36.002304
45.002304	45	45.002304
54.0023041	54	54.002304
63.0023042	63	63.002304
72.0023043	72	72.002304
81.0023043	81	81.002304
90.0023043	90	90.002304
99.0023043	99	99.002304
108.0023043	108	108.002304
117.0023042	117	117.002304
126.0023041	126	126.002304
135.002304	135	135.002304
144.0023039	144	144.002304
153.0023038	153	153.002304
162.0023037	162	162.002304
171.0023037	171	171.002304
180.0023037	180	180.002304
189.0023037	189	189.002304
198.0023037	198	198.002304
207.0023038	207	207.002304
216.0023039	216	216.002304
225.002304	225	225.002304
234.0023041	234	234.002304
243.0023042	243	243.002304
252.0023043	252	252.002304
261.0023043	261	261.002304
270.0023043	270	270.002304
279.0023043	279	279.002304
288.0023043	288	288.002304
297.0023042	297	297.002304
306.0023041	306	306.002304
315.002304	315	315.002304
324.0023039	324	324.002304
333.0023038	333	333.002304
342.0023037	342	342.002304
351.0023037	351	351.002304

Define:

$$\delta\text{Residual}(D) := D + \text{acc} - \left[1 - \left(\frac{\text{PHI}(D)}{360}\right)\right]$$

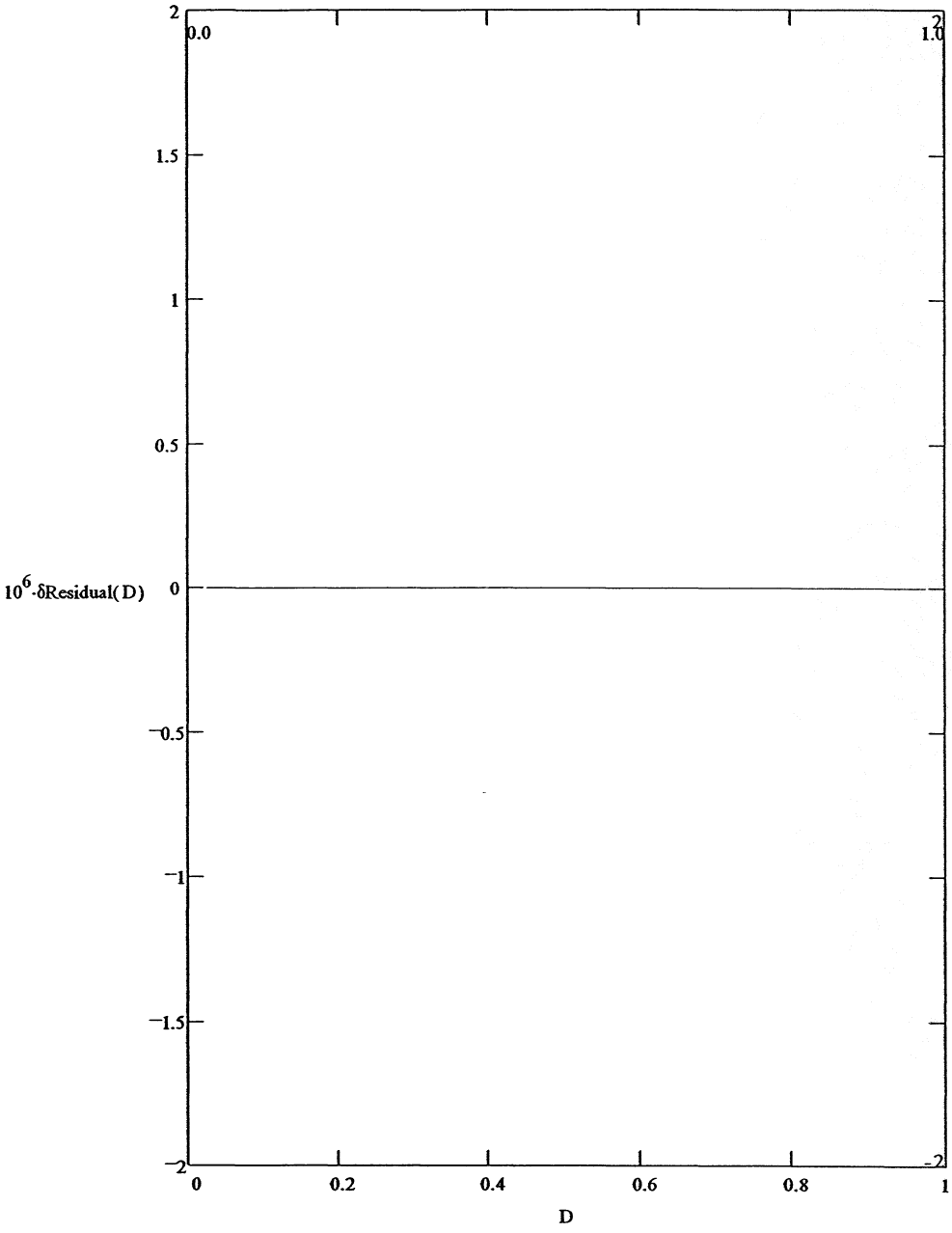

Appendix I. Range Scan Programs.

In this appendix we suggest a method to define and generate the scenarios demanded of the GBT rangefinder metrology system.

In each case, a measurement problem is defined. The measurements needed to solve that problem are defined, together with procedures for implementing the measurements. Correction, reduction, adjustment and analysis procedures for processing the measured range data are outlined.

To define a measurement program, in general, we carry out the following steps:

1. Define the measurement problem.
2. Define the required calibration and refractometer scans.
3. Define and list the sets of rangefinders and targets to be employed.
4. Define the sequence of rangefinder measurement scans and calibration scans.
5. Define the required telescope input signals. These might be, e.g.: commanded azimuth encoder, commanded elevation encoder, commanded Stewart platform position state vectors, scan program clock starting time.
6. Select scan integration times: Δt_i for ordinary range scans, $(\Delta t_i)_{refr}$ for refractometer range scans, $(\Delta t_i)_{comp}$ for rangefinder calibration scans.
7. Define the method of selecting the scan program start time, t^0.
8. Inner and outer scan loop cycle periods, Δt_{cyt} and Δt_{cy} , are selected, with their scan number multiplicities, $1 + (m_{\max})_{ij}$ and $1 + p\max$.
9. Select a mid-scan time, t_{ij}^{00} , for each pair {Rangefinder ZY_i , Target T_j}.
10. Select a mid-scan time, $(t_{ij}^{00})_{refr}$, for each refractometer range scan.
11. Select a mid-scan time, $(t_{ii}^{00})_{comp}$, for each rangefinder range scan.
12. Provide allotted inter-scan time intervals for rangefinder aiming and motion drive Δt_{md} , and handshaking Δt_{hs} to notify scan readiness and acknowledge permission for start of illumination.

13. Define algorithms and data handling for of line-of -sight visibility computations for each scan.

14. Define the data handling for updating the scan sequence list, to eliminate range pairs without line-of-sight visibility.

15. Provide algorithms for computing local rangefinder counts to aim each scan.

16. Define command instructions for performing the scans.

17. Define all scan program option switch settings.

18. Define the data logging protocols.

19. Provide algorithms and data handling for computations of relative radial velocity of rangefinder and target.

20. Specify all corrections to the range data, for the program. These include corrections for: refraction (as determined e.g. from multiple refractometer range measurements), calibration reference path, prism correction constant and depth, illumination incidence angle on target retroreflector, relative radial velocity of rangefinder and target.

21. Provide algorithms for reduction of range data.

22. Define needed range interpolations and extrapolations.

23. Provide command instructions and codes for performing range interpolations and extrapolations.

24. Define any required range adjustments, trilaterations, extrapolated or interpolated trilaterations, and coordinate determinations.

25. Specify data logging protocols for adjusted ranges and coordinates.

26. Calculate main reflector surface point coordinates from adjusted surface reflector coordinates, in surface measurement programs.

27. Specify command instructions for distribution of analyzed and processed measurement data.

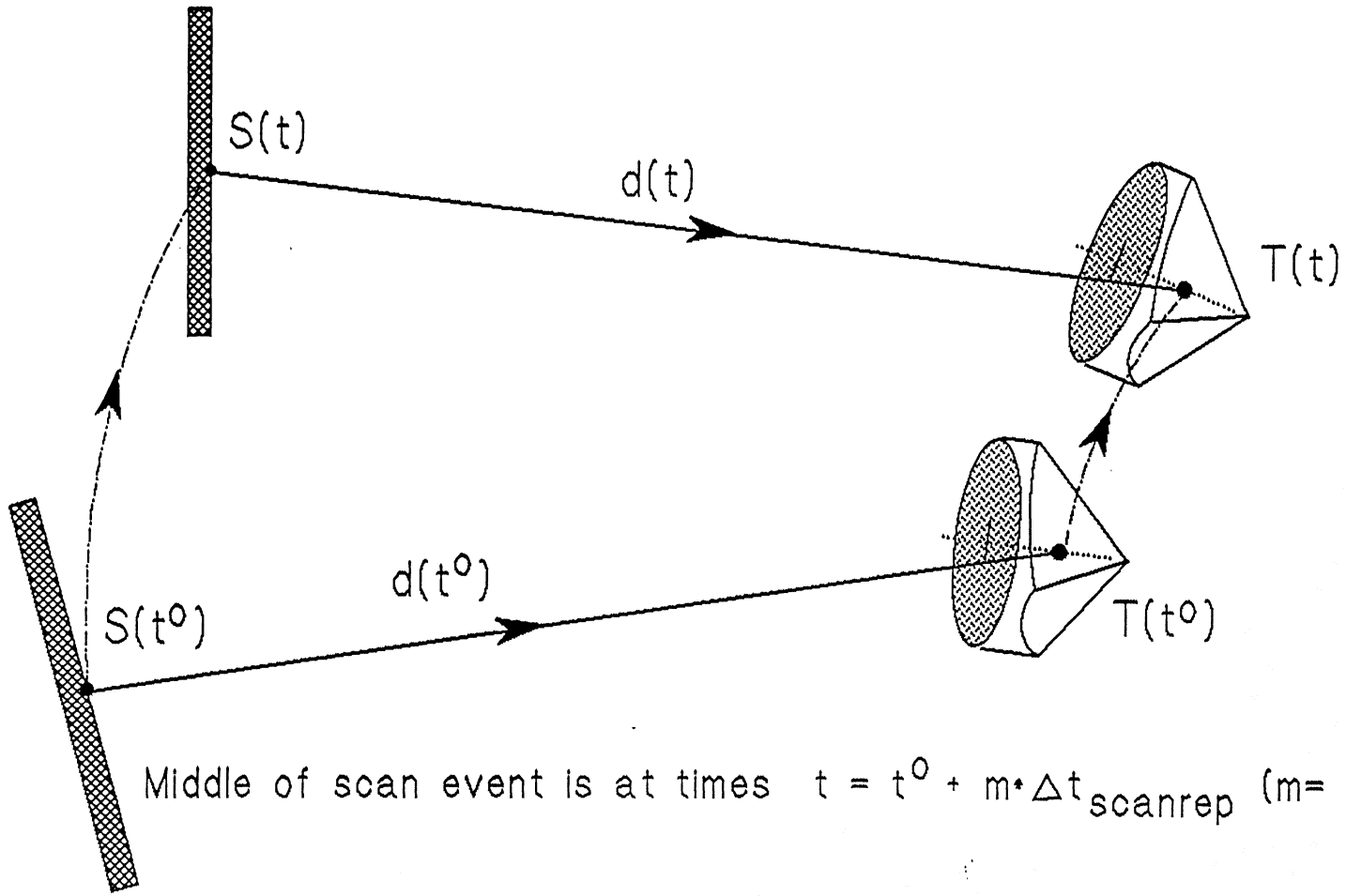

Middle of scan event is at times $t = t^{o} + m \cdot \Delta t_{scanrep}$ $(m = 0,1,\ldots,m_{max})$.

Individual laser scan interval on target = $\Delta t_{integration}$ for each scan event.

Figure 1. Dynamic Range Measurement For A Scan-Point/Target Pair

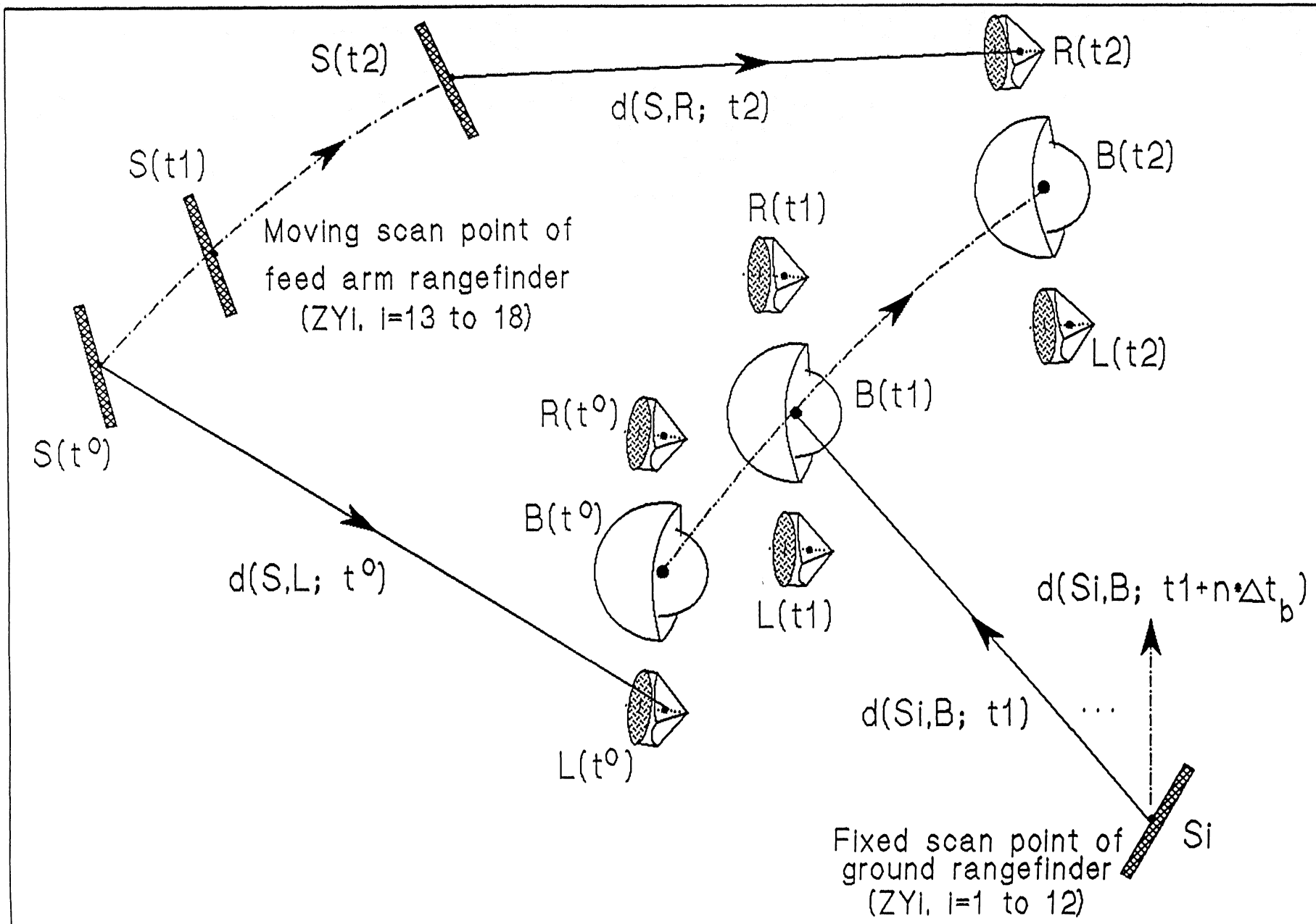

Figure 2. Dynamic Range Measurement For A Scan-Point/Retrosphere Pair

$$t_{ij} = t_{ij}^{o} + m_{ij} \cdot h_{ij} = t_{ij}(m_{ij})$$

$$(m_{ij} = 0, \ldots, m_{ij\,max})$$

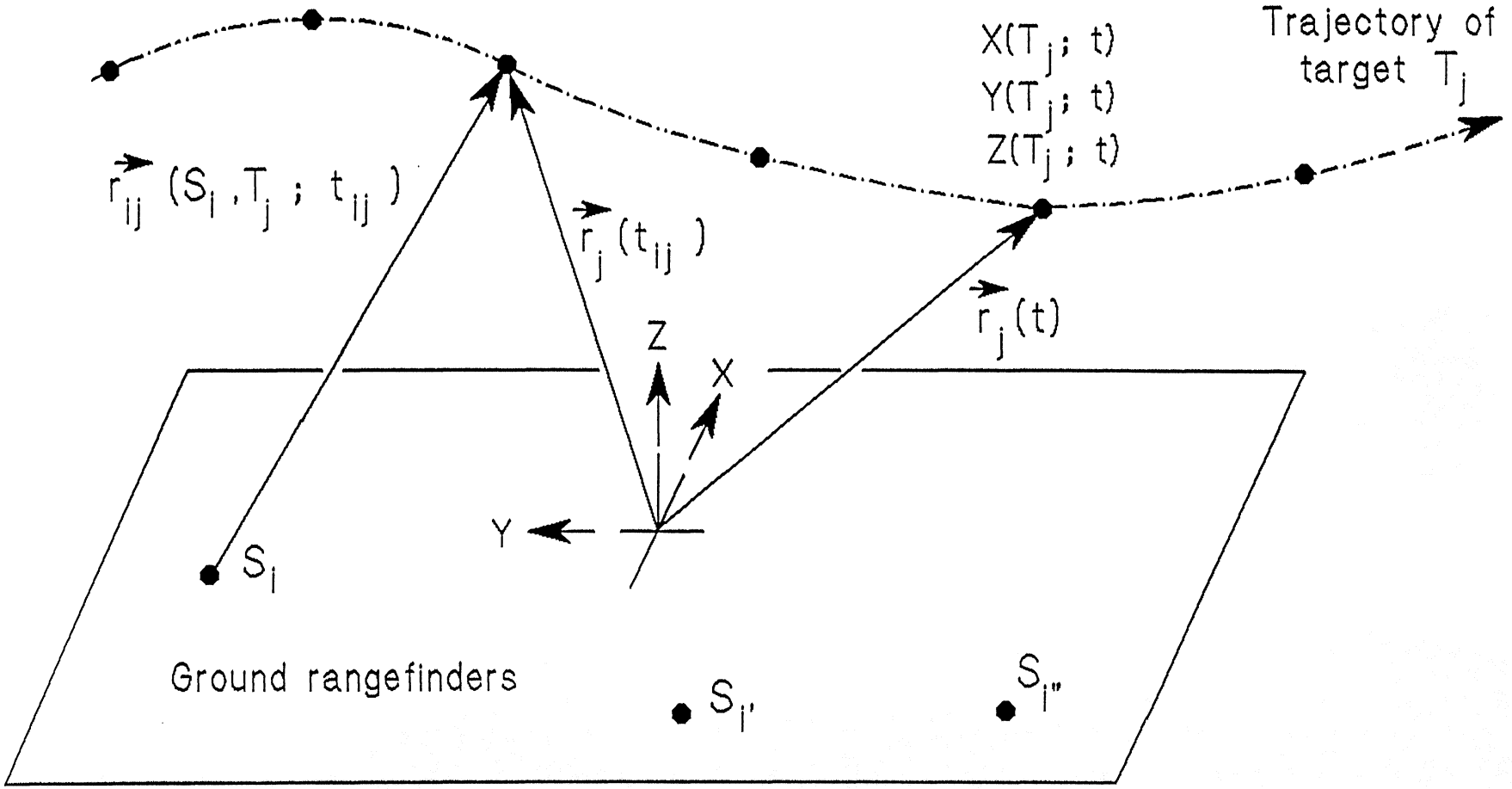

Figure 3. The Dynamical Position Computation Problem For Ground Ranging.

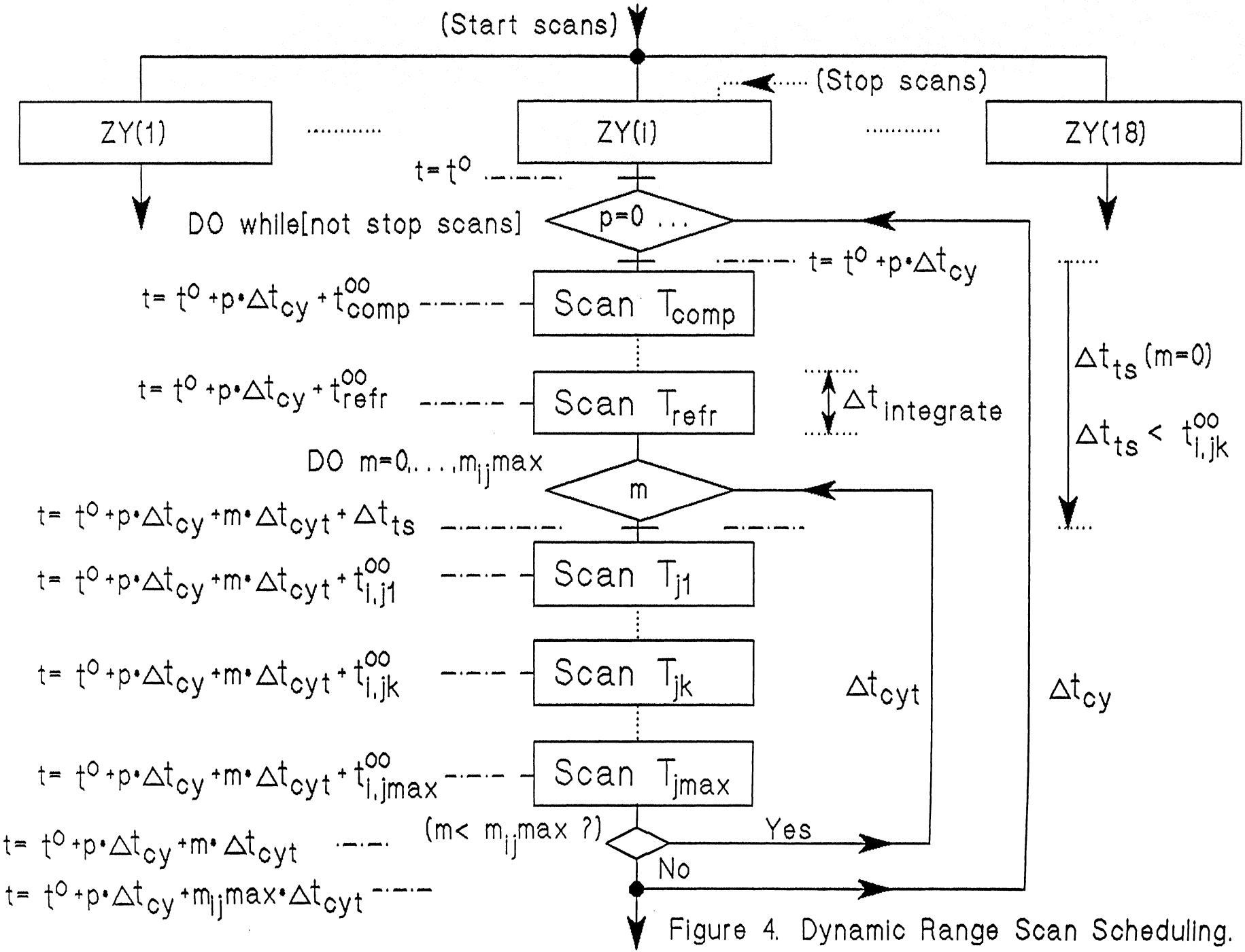

Figure 4. Dynamic Range Scan Scheduling.

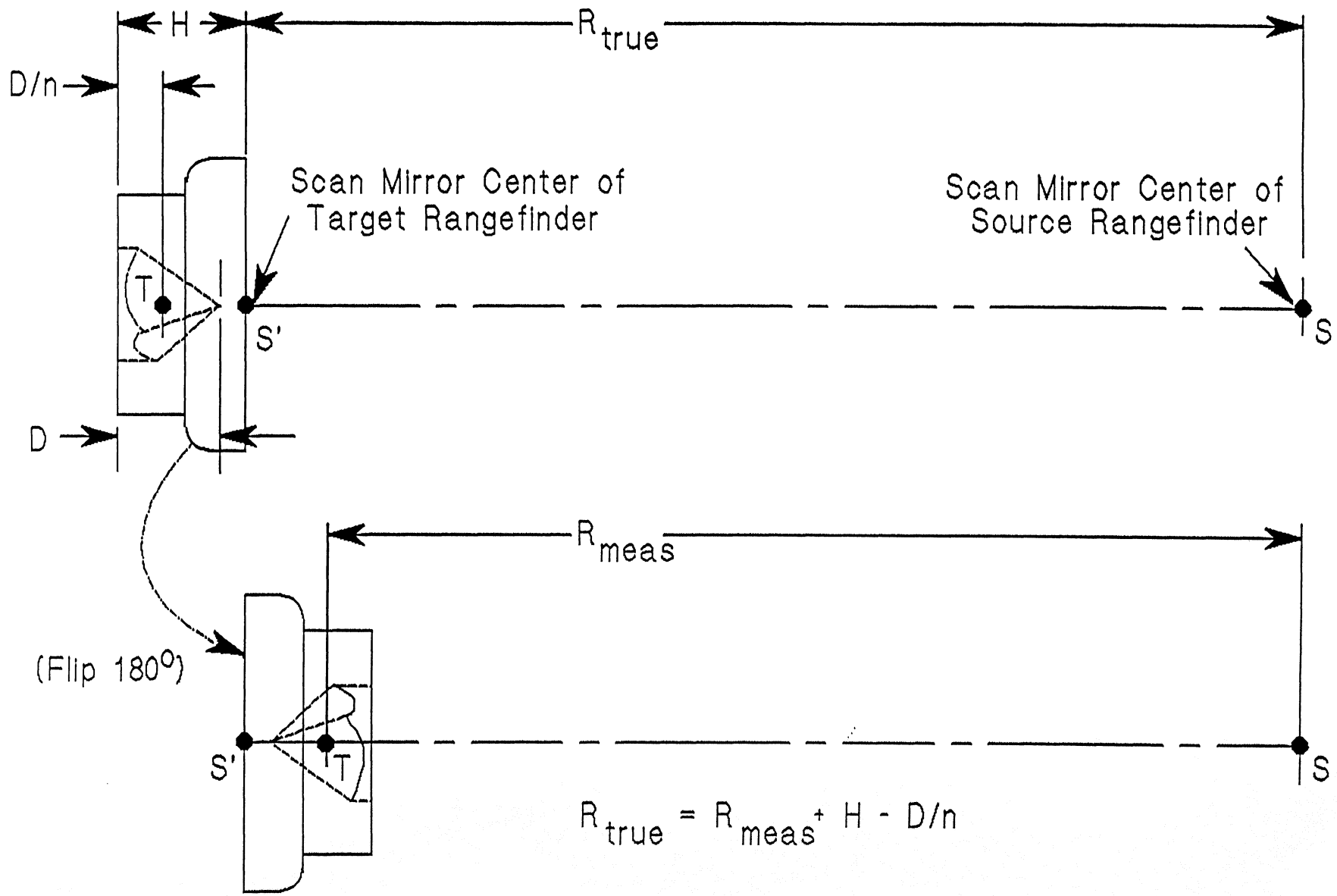

Figure 5. Rangefinder-To-Rangefinder Range Measurement, Using A Retro-Prism On The Back Of A scan Mirror.

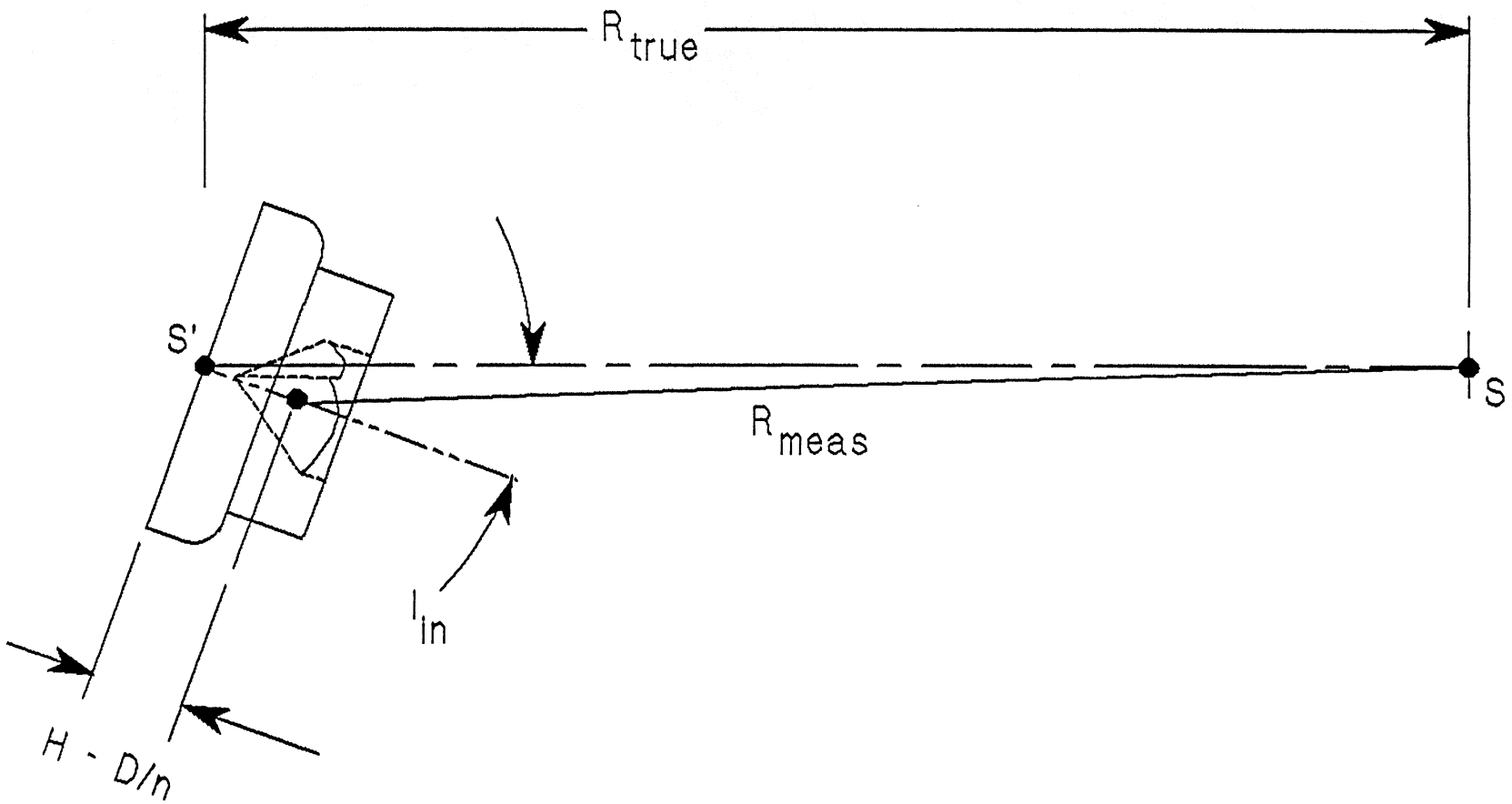

Figure 6. Rangefinder-To-Rangefinder Range Measurement At Oblique Incidence

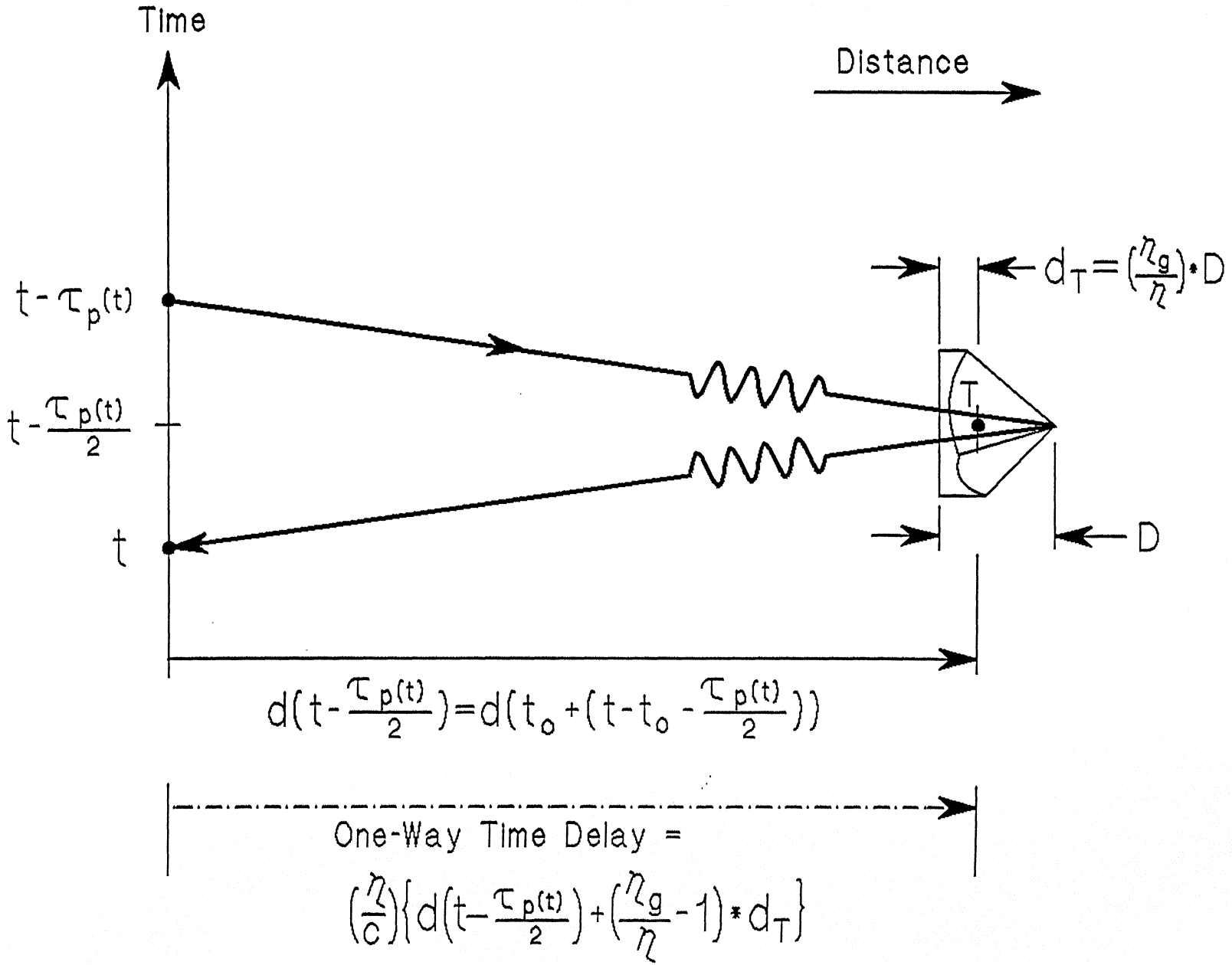

Figure 7. Propagation Delay In Ranging.

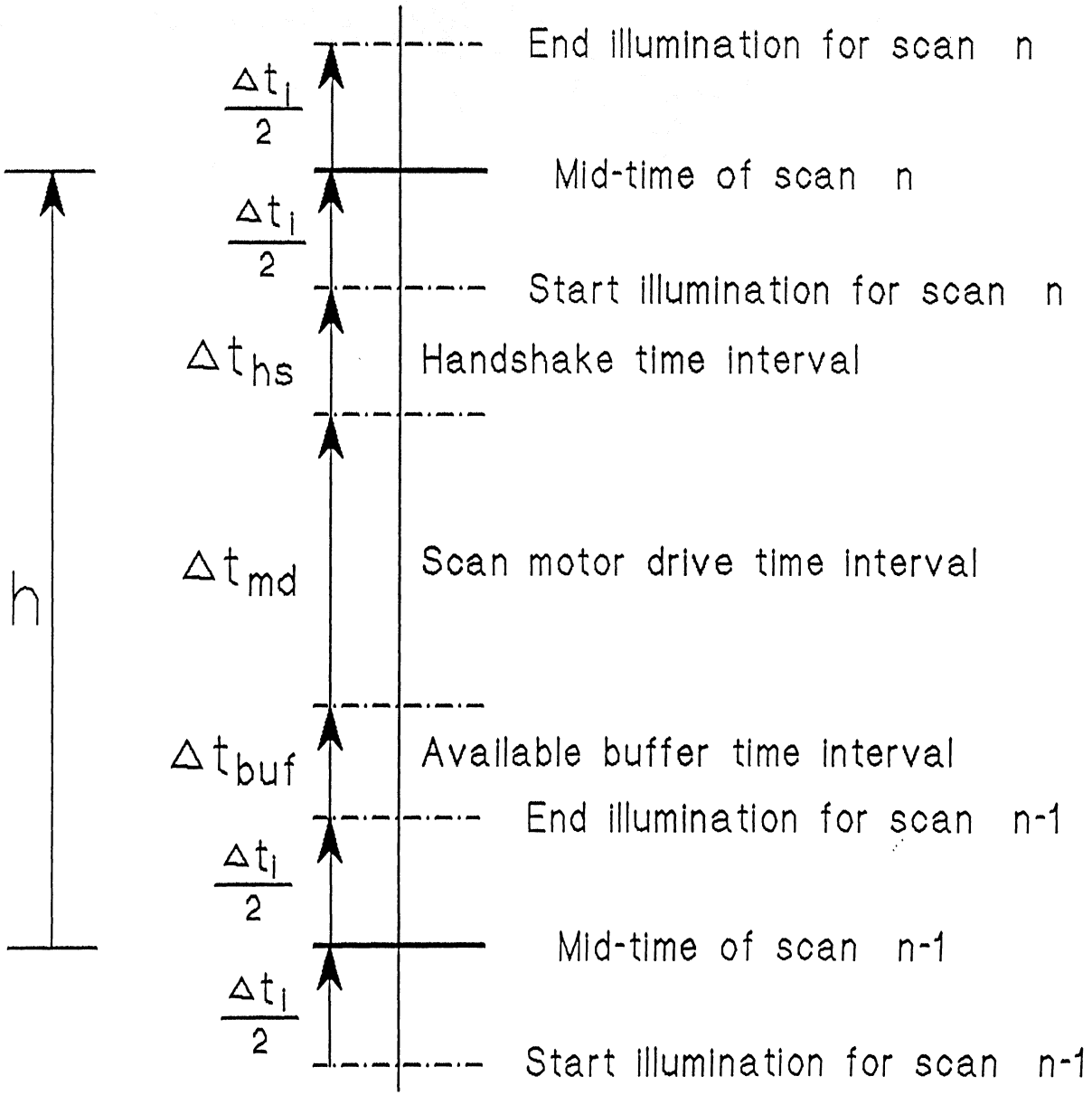

Figure 8. Scan Events Between Successive ZY_i Scans.

Range distance decreases with increasing phase:

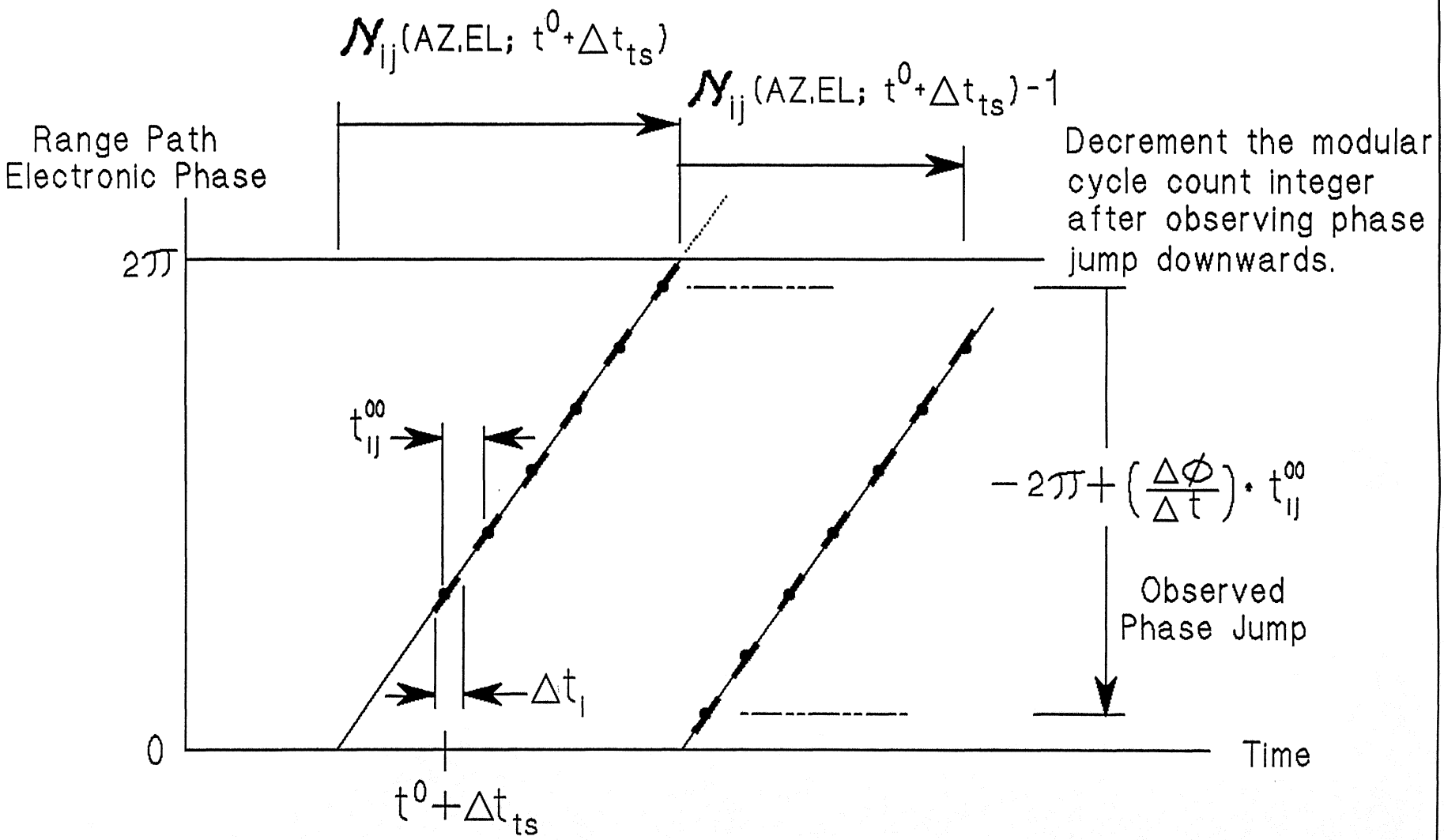

Figure 9a. Change Of Modular Range Integer To Account For Phase Cycle Slip Downwards.

Range distance increases with decreasing phase:

Increment the modular cycle count integer after observing phase jump upwards.

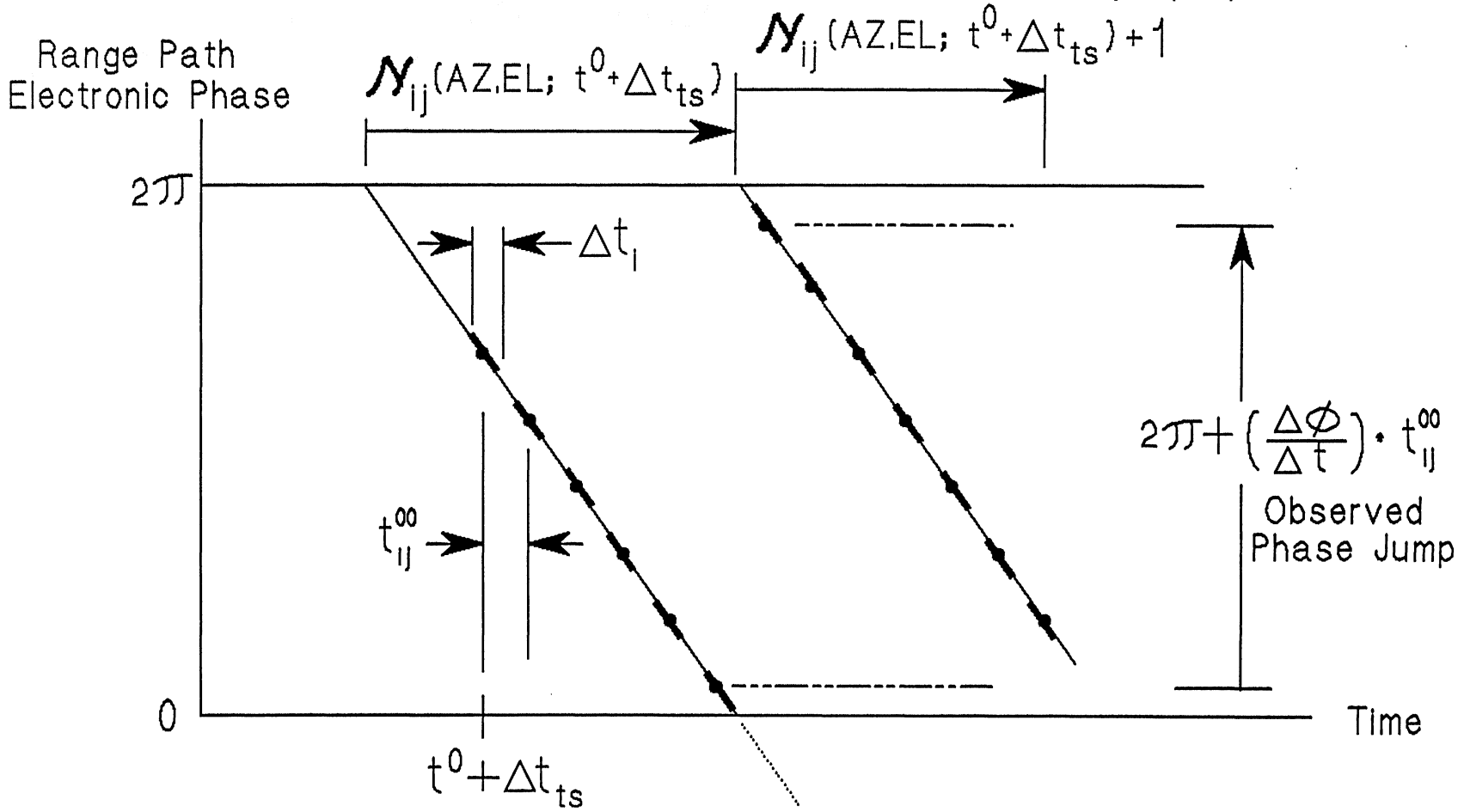

Figure 9b. Change Of Modular Range Integer To Account For Phase Cycle Slip Upwards.